Masters Theses   Graduate School

5-2004

Combination of *Bcr-Abl*-specific RNA Interference with Imatinib Treatment in the K-562 Cell Line

Benjamin Eugene Baker
University of Tennessee, Knoxville

www.manaraa.com

To the Graduate Council:

I am submitting herewith a thesis written by Benjamin Eugene Baker entitled "Combination of *Bcr-Abl*-specific RNA Interference with Imatinib Treatment in the K-562 Cell Line." I have examined the final electronic copy of this thesis for form and content and recommend that it be accepted in partial fulfillment of the requirements for the degree of Master of Science, with a major in Comparative and Experimental Medicine.

Albert T. Ichiki, Major Professor

We have read this thesis and recommend its acceptance:

Robert L. Donnell, Daniel P. Kestler, Karla J. Matteson
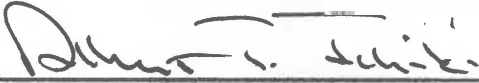
Accepted for the Council:
Carolyn R. Hodges

Vice Provost and Dean of the Graduate School

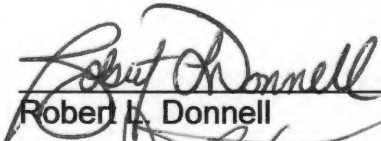(Original signatures are on file with official student records.)

To the Graduate Council:

I am submitting herewith a thesis written by Benjamin Eugene Baker entitled "Combination of *Bcr-Abl*-specific RNA Interference with Imatinib Treatment in the K-562 Cell Line." I have examined the final paper copy of this thesis for form and content and recommend that it be accepted in partial fulfillment of the requirements for the degree of Master of Science, with a major in Comparative and Experimental Medicine.
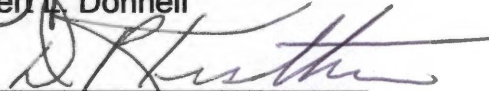
Albert T. Ichiki, Major Professor

We have read this thesis
and recommend its acceptance:

Robert L. Donnell
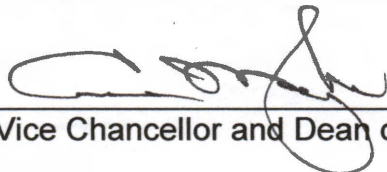
Daniel P. Kestler

Karla J. Matteson

Accepted for the Council:

Vice Chancellor and Dean of Graduate Studies

Combination of *Bcr-Abl*-specific RNA Interference with

Imatinib Treatment in the K-562 cell line

A Thesis Presented for the Master of Science Degree

The University of Tennessee, Knoxville

Benjamin Eugene Baker

May 2004

Dedication

To my Wife and my Mother,

for their unending love and encouragement.

Acknowledgements

I am deeply grateful for the patience, support and opportunity that my mentor and friend, Dr. Albert Ichiki, extended to me. His guidance taught me the discipline and art of science.

I would like to express my appreciation to the other members of my committee, Dr. Dan Kestler, Dr. Karla Matteson, and Dr. Bob Donnell. Their advice and direction was integral in my development as a scientist.

I would like to express my deepest gratitude to my family, especially my wife, Erin, who has offered support and encouragement throughout my graduate education. I would also like to thank my mother, Willie, who has sacrificed so much for my education and has always pushed me to excel.

Abstract

RNA interference (RNAi) involves the specific repression of the translation of a gene through mRNA degradation. Its application has been extended to a variety of studies both *in vitro* and *in vivo*. The *Bcr-Abl* translocation is the cytogenetic marker for chronic myelogenous leukemia (CML) and has been studied extensively. The K-562 cell line possesses the *Bcr-Abl* fusion gene and has been established as a model for RNAi. Imatinib mesylate (Gleevec) is a proven specific inhibitor of the Bcr-Abl tyrosine kinase. The aim of this study was to combine K-562 cells primed with short interfering RNA (siRNA) targeting the *Bcr-Abl* fusion site with treatment with Gleevec. Two different preparations of siRNA: homogenous-synthetic *Bcr-Abl* and heterogeneous-transcribed-digested *Bcr-Abl* were used to silence the *Bcr-Abl* fusion gene. The synthetic siRNA consisted of a homogenous mixture of 21nt long double stranded RNA duplexes specific for the *Bcr-Abl* fusion site. The transcribed-digested *Bcr-Abl* siRNA were generated using an in vitro transcription method producing a 450 bp cloned fragment with the *Bcr-Abl* fusion site in the center of the cloned region. This cloned fragment was further digested with RNAse III to produce a heterogeneous mixture of *Bcr-Abl* 19-21nt siRNA duplexes. We demonstrated a 70% down-regulation of the *Bcr-Abl* mRNA through real time PCR and RT-PCR as well as a 75% down-regulation of the Bcr-Abl and Bcl-$_{XL}$ proteins in K-562 cells transfected with synthetic *Bcr-Abl* siRNA. The IC_{50} of Gleevec alone in the K-562 subline F_1 was lowered from $0.2\mu M$ to $0.06\mu M$ in cells transfected with both preparations of *Bcr-Abl* siRNA, while no effect was observed in an irrelevant siRNA control. This

suggests an additive relationship between Gleevec and *Bcr-Abl*-specific-siRNA treated cells. An increase in apoptosis was also seen in K-562 cells primed with *Bcr-Abl* siRNA and treated with Gleevec indicating the additive relationship between Gleevec and *Bcr-Abl* siRNA. These results indicate that priming K-562 cells with *Bcr-Abl* siRNA correlate with a decrease in the effective dose of Gleevec required to inhibit the Bcr-Abl protein.

Table of Contents

List of Figures

List of Abbreviations

Abl: Abelson oncogene

ABD: Abl binding domain

AS: antisense

Bcr: breakpoint cluster region

CML: chronic myelogenous leukemia

DMEM: Dulbecco's modified Eagle's medium

FACS: fluorescence activated cell sorter

FBS: fetal bovine serum

FITC: fluorescein isothiocyanate

Ig: immunoglobulin

IL: interleukin

JAK: janus activated kinase

MAP: mitogen activated protein

MEK: MAP Erk Kinase

OD: oligomerization domain

PBS: phosphate buffered saline

PCR: polymerase chain reaction

PI3K: phosphitidylinositol triphosphate kinase

Ph: Philadelphia chromosome

PTGS: post transcriptional gene silencing

RNAi: RNA interference

RT-PCR: reverse-transcriptase polymerase chain reaction

shRNA: short hairpin RNA

siRNA: short interfering RNA

STAT5: signal transducer and activator of transcription-5

TNF-α: tumor necrosis factor-alpha

Chapter 1

Review of the Literature

Introduction

RNA interference (RNAi) is a pathway that targets specific transcripts and results in gene-specific silencing (1-9). The ability to target and interfere with specific RNA has been used in a variety of studies ranging from gene modulation to screening for specific gene function and disease intervention (10-13). The potency and efficacy of RNAi surpasses other known methods of transcriptional down-regulation such as antisense and has a longer sustained effect of transcriptional repression (14-16). Recently, focus has been placed on the delivery of RNAi, for which there have been significant advances making the application of RNAi attainable for both *in vitro* and *in vivo* applications (17, 18). RNAi promises to revolutionize genetics by providing the ability to knock down the expression of any gene (19, 20).

In chronic myelogenous leukemia, (CML) the molecular marker of malignancy is the presence of the breakpoint-cluster-region/Ableson (*Bcr-Abl*) oncogene (21-23). This marker is not present in normal cells and the Abl transcript and polypeptide are highly restricted in their expression (24). Therefore, the *Bcr-Abl* fusion gene is an ideal target for RNAi analysis and therapy (25, 26). The K-562 cell line is a CML derivative that expresses high levels of the *Bcr-Abl* fusion gene, making it a rigorous model for *in vitro* studies of

1

RNAi (27). To date, various forms of RNAi have been applied *in vitro* in studies using various cell lines, including K-562 (28-31).

Imatinib mesylate (Gleevec) is a specific tyrosine kinase inhibitor that targets the Bcr-Abl oncoprotein (32-37). It has had success used as a clinical therapeutic agent for CML (36). Bcr-Abl confers resistance to apoptosis; thus, inhibition of Bcr-Abl with agents such as Gleevec renders cells susceptible to apoptosis (37, 38). Gleevec has been shown to inhibit the proliferation of K-562 cells and, eventually, lead to differentiation, apoptosis and cell death *in vitro* (34, 37, 39). Gleevec shows synergism when administered in conjunction with a number of different agents, including interferon-α, etoposide, and daunorubicin in K-562 cells (40, 41). This observation supports the focus of this study, which is to investigate possible synergistic effects of the combination of with Bcr-Abl-RNAi with Gleevec using K-562 cells. Thus, targeting the protein substrate-binding site of the Bcr-Abl protein in tandem with the *Bcr-Abl* transcript provides two separate methods of inhibition for the same molecular target.

Chronic Myelogenous Leukemia

Chronic myelogenous leukemia (CML) presents with elevated levels of myeloid and erythroid cells in peripheral blood and with marked myeloid hyperplasia in the bone marrow (21). The disease exhibits three phases: the chronic phase, lasting 3 to 5 years; the accelerated phase, with marked hypermetabolism and intramedullary expansion of leukemic cells; and blast

crisis, confirmed by greater than 30% blasts in the peripheral blood and/or bone marrow (42).

CML is a clonal hematopoietic malignancy identified by the Philadelphia (Ph) chromosome, which is found in 95% of CML patients (22, 43). The Ph chromosome results from the t(9q34;22q11) translocation, where the 5' end of the Abelson (c-abl) gene from chromosome 9 is relocated onto the 3' end of the Breakpoint cluster region (c-bcr) gene on chromosome 22 in a head to tail manner (43).The Ph chromosome was the earliest specific chromosome rearrangement identified in a malignancy and has been cloned and characterized at the molecular level (23, 44). The cytogenetic evolution pattern correlates with the clinical behavior of a disease (44).

Bcr-Abl Fusion

The t(9q34;22q11) translocation results in the chimeric gene, Bcr-Abl, which is transcribed into an 8.5 kb hybrid mRNA, and translated into the Bcr-Abl fusion protein (Figure 1) (45). The breakpoint in the Abl gene can occur anywhere within the 300kb 5'end of the gene, upstream of the first alternative exon Ib, between exons Ib and Ia, or downstream of exon Ia (46). In contrast, the vast majority of CML patients possess a breakpoint in the Bcr gene within a 5.8kb region known as the major breakpoint cluster region (M-bcr), spanning 5 exons from exons 12 to 16, referred to as b1 to b5 (24, 46-48).

The Bcr-Abl fusion protein is a constitutively activated cytoplasmic tyrosine kinase of 210 kD, 902 amino acids in length, and is complexed in vivo with both
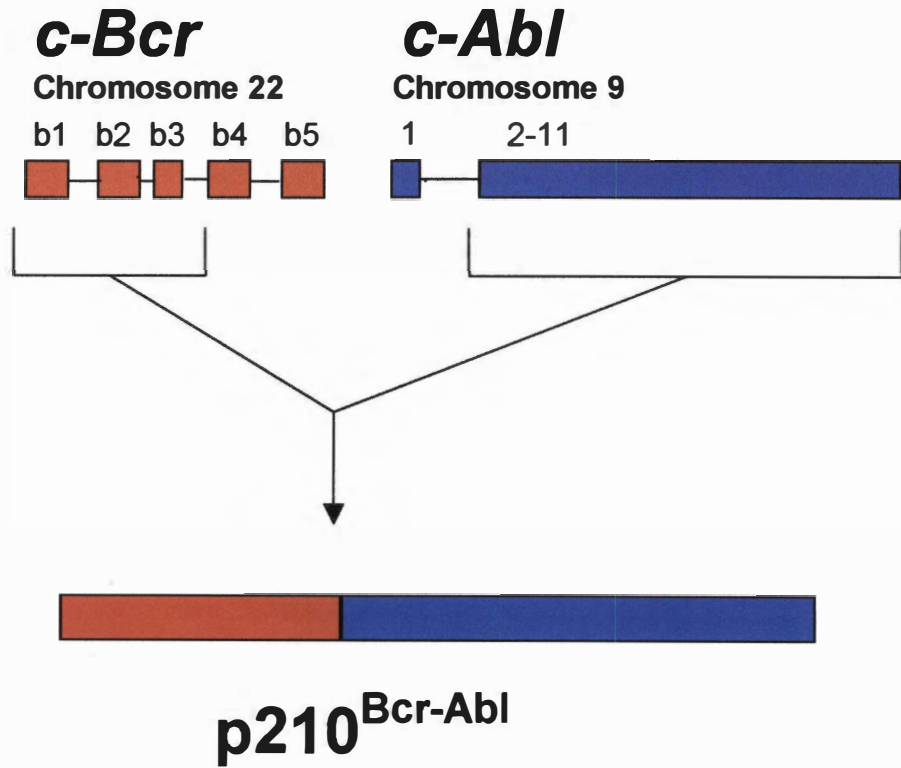
Figure 1. The Bcr-Abl fusion protein. The origin of the Bcr-Abl fusion protein, the Philadelphia chromosome, results from the translocation of *c-Bcr* from chromosome 22 onto *c-Abl* located on chromosome 9 in a head to tail manner.

p160 Bcr and ph-P53 proteins (21, 49, 50). Protein tyrosine kinases are members of a group of enzymes that bind ATP and catalyze the transfer of the γ-phosphate to the hydroxy group of a tyrosine residue on a protein (32). The phosphorylated substrates can then serve as binding sites for other substrates, carrying out the signal transduction cascade of a variety of pathways (32).

Many intracellular pathways are directly affected by the expression of the Bcr-Abl protein (Figure 2) (51). The substrates targeted by Bcr-Abl include CRKL, p62Dok, paxillin, CBL and RIN, which are integral in pathways involving PI3-kinase, Akt, ERK JUN kinase, MAP, Myc, STAT, and Ras/Raf (21, 52-54). Bcr-Abl initiates the Ras/Raf/MEK/ERK, JAK/STAT, PI3K/Akt signal transduction pathways, resulting in cell proliferation (51, 55, 56).

Bcr-Abl fusion in hematopoietic cell lines abrogates their dependency on growth factors for proliferation and survival (54). The constitutive tyrosine kinase activity of the nascent Bcr-Abl oncoprotein provides the transforming ability (57, 140). The expression of Bcr-Abl in mice induces a disease similar to CML, which corroborated the role of Bcr-Abl as a transforming agent of malignancy (50).

Although the role of the Bcr gene is not fully understood, it is expressed ubiquitously, with the highest mRNA levels found in the brain and hematopoietic cells (24). Bcr protein levels are elevated in the early stages of myeloid differentiation, and levels dropped significantly as cells mature to polymorphonuclear leukocytes (24). The Bcr protein has also been linked to cytoskeletal reorganization, and DNA repair (24). While the intracellular role of
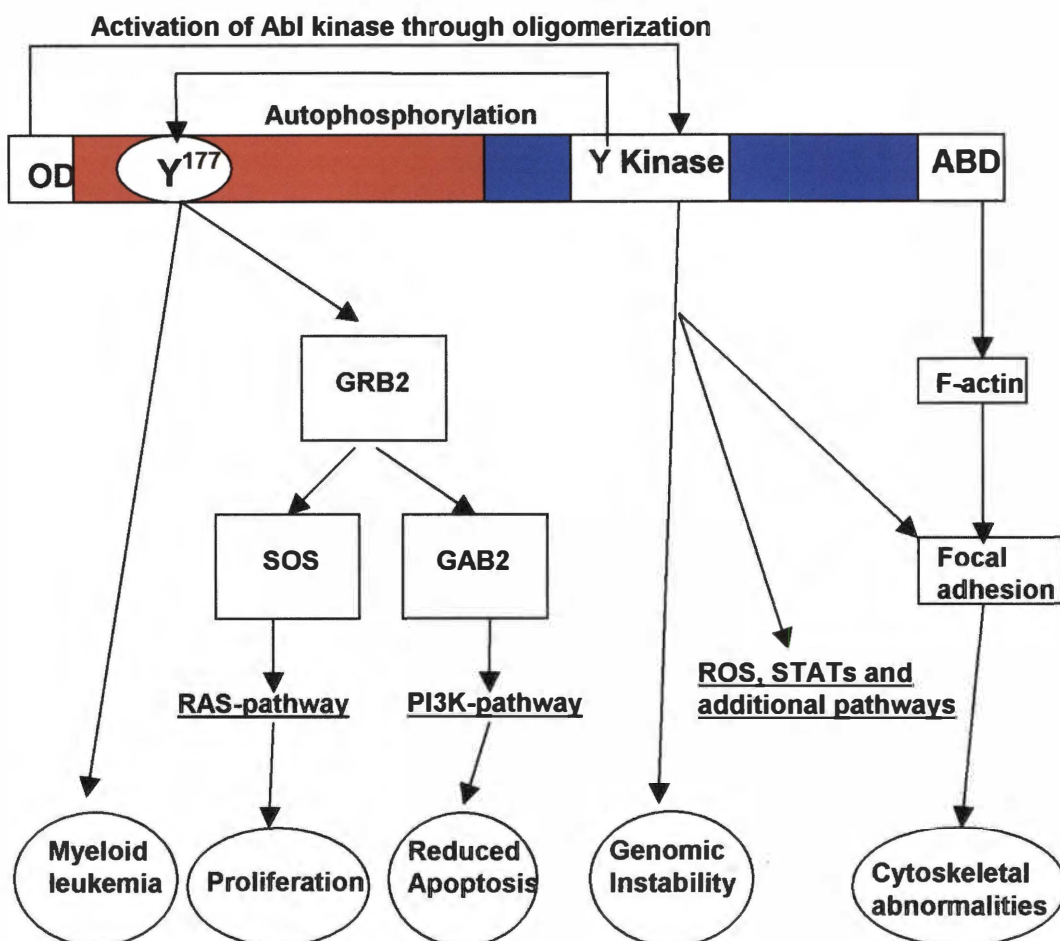
Figure 2. Bcr-Abl pathway interactions. The expression of Bcr-Abl modulates the Ras/Raf, PI3K, Jak/STAT and MEK/ERK pathways, leading to multiple proliferative and antiapoptotic outcomes. Bcr-Abl activation follows the binding of the oligomerization domain in the Bcr protein onto the tyrosine kinase region of the Abl protein. The Abl protein then phosphorylates Tyr[177] in the Bcr protein leading to proliferation.

Bcr has not been determined in normal cells, its suggested function in CML cells is as a negative regulator of Bcr-Abl kinase activity (58). The removal of the oligomerization domain, the first 63 amino acid residues of the Bcr serine/threonine kinase, results in a truncated Bcr moiety resistant to autophosphorylation by the activated Abl tyrosine kinase and limited transforming ability (24, 57, 58). This truncated Bcr protein strongly inhibits the Bcr-Abl kinase activity (58). Arlinghaus *et al.* demonstrated Bcr-Abl inactivating normal Bcr through phosphorylation (58). This observation supports the role of the activated Bcr kinase as inhibiting the Bcr-Abl kinase and asserts the function of Bcr-Abl as deactivating the Bcr serine/threonine kinase, propagating the deregulation of the Bcr-Abl tyrosine kinase activity (58). The normal function of the Abl protein is primarily as a tyrosine kinase, and Abl is differentially phosphorylated during the cell cycle (24, 59, 60). Abl associates with cell cycle proteins Rb, p53, p73, Atm, and cyclin D and overexpression of Abl leads to growth arrest (24, 45). Since normal cells lack the Bcr-Abl fusion protein, it represents a selective site for intervention (32).

K-562 Cell Line

The K-562 cell line is an undifferentiated leukemic line derived from the plural effusion of a CML patient in blast crisis (61, 62). These cells were first observed to maintain their Philadelphia chromosome positive, Ph (+), status through 175 serial passages over 3 ½ years (61). In 1975, 1-4 Ph chromosomes were detected in each cell (61). Several atypical Ph chromosomes, common in

K-562 cells, result in an increased amount of Bcr-Abl oncogene expression (27, 63). When compared to standard patient samples, K-562 cells were reported to have a 82-fold overproduction of the Bcr-Abl transcript in 1994 and a 200-fold overproduction of the Bcr-Abl transcript in 1997 (27). In the K-562 cell line, the fusion site of the Bcr-Abl gene is between the Bcr exons b3 and b4 and between the Abl exons a1 and a2, resulting in the b3a2 variant (46). Expression of Bcr-Abl by the K-562 cell line was found to impart resistance to apoptosis induction in response to various cytotoxic drugs or serum deprivation (52).

Gleevec

STI-571 (imatinib mesylate, or Gleevec) (Figure 3) is a *Bcr-Abl-* specific tyrosine kinase inhibitor (32, 64). Gleevec has been termed the "gold standard" in treatment of chronic myelogenous leukemia due to its specificity (36, 65, 66). The Bcr-Abl protein is a cytosolic tyrosine kinase that does not depend on ligand binding and subsequent receptor dimerization for activation (32). This aspect of *Bcr-Abl* results in an inability to modulate its activity with receptor-based inhibitors (32). The limited sequence variation surrounding the ATP-binding site, as well as the conformational differences between inactive and active forms of kinases, offer sources for inhibition (67). Gleevec works as an ATP-competitive inhibitor of the *Bcr-Abl* kinase activity (32). From the crystal structure, it was shown that Gleevec binds to *c-Abl* via a series of H-bond interactions and van der Waals contacts with specific amino acid residues (32). Mutations in these amino acids result in resistance to Gleevec (32). While Gleevec is a potent

8
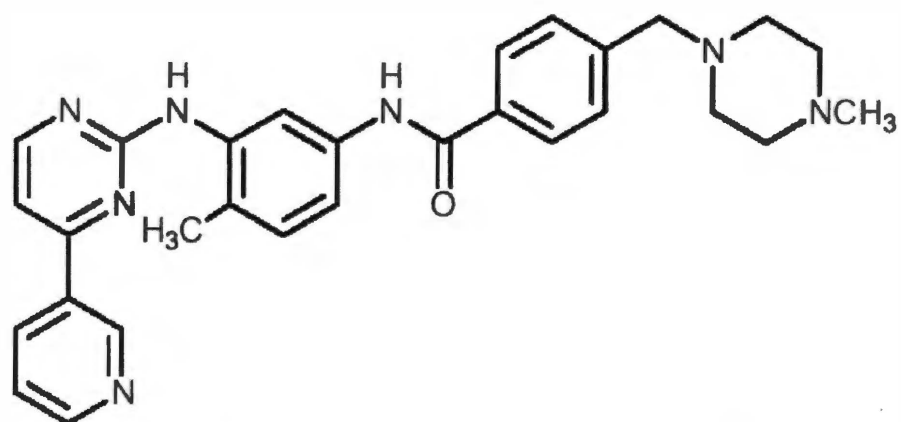
STI-571(a.k.a. imatinib or Gleevec®)

Figure 3. Structure of Gleevec. imatinib mesylate or Gleevec has a relative molecular mass of 589.7 with a molecular formula of $C_{29}H_{31}N_7O$ • CH_4SO_3 and a chemical formula 4-[(4-Methyl-1-piperazinyl) methyl]-N-[4-methyl-3-[[4-(3-pyridinyl)-2-pyrimidinyl] amino]-phenyl] benzamide methanesulfonate. Figure from Novartis (32).

competitive inhibitor of *c-Abl*, and also interferes with *c-Kit* and PDGFR-β, it is inactive against any other tyrosine kinases (32).

In vitro studies of Gleevec, using Bcr-Abl-expressing cell lines including K-562, have demonstrated an antiproliferative effect (33, 68, 69). Gleevec kills leukemic cells *in vitro* and *in vivo* through an apoptosis-mediated mechanism (34, 68, 70). Apoptosis was detected measuring caspase 3 activity and the release of cytochrome c from the mitochondria, which are both hallmarks of apoptosis (34, 68, 71). The apoptotic mechanism that Gleevec triggers involves the downstream inactivation of the Bcl-2 family protein, Bcl_{-XL} (34, 39, 72). This protein is also constituitively activated through autophosphorylation by Bcr-Abl (39). Oetzel *et al.* showed that Gleevec caused the downregulation of Bcl_{-XL}, resulting in susceptibility to programmed cell death, while there was no change in the level of Bcl-2 (34). Gleevec also mediated a decrease in Akt kinase activity and an increase in the Apo-2L/TRAIL-induced apoptosis of K-562 cells (73).

Although Gleevec has specificity and efficacy, the required length of the treatment, which may be extended for the length of a person's life, can result in the development of resistant clones (73-76). There is evidence of a number of mechanisms responsible for the development of Gleevec-resistant CML clones, such as increased production of the Bcr-Abl transcript number, increases in the expression of the Bcr-Abl protein, point mutations in the ATP binding pocket or other functional sites, and increased drug efflux (32, 74, 77-80).

Gene Silencing

Gene silencing is defined as the silencing of the translation of a specific gene (19, 81). This concept has been applied successfully both *in vitro* and *in vivo* (1, 2, 10, 18, 19, 82). Antisense technology has been applied over the past decade with some success (14, 83, 84). Antisense interference involves either antisense DNA (oligodeoxynucleotides, ODN) or RNA homologous to the specific region of the mRNA (14). These ODNs are transfected into cells and subsequently hybridize to the specific region within a particular mRNA transcript (14). This binding inhibits translation of the message (14). Antisense interference is related to RNAi, which also specifically targets mRNA (14, 85). It is noteworthy that the stability of single-stranded antisense ODNs is considerably less than that of double stranded RNA, which results in less efficient silencing (28).

New evidence supports multiple functions for gene silencing in a variety of biological processes, including antiviral defense, embryonic development, and maintenance of genomic stability (86-89). Gene silencing is referred to as RNAi in animals, post-transcriptional gene silencing (PTGS) or co-suppression in plants and quelling in fungi (86, 90, 91). Although the processes share some similar steps and result in specific targeting of mRNA, there are distinctive differences in the proteins involved, the length of the effect, and the ability to exhibit gene repression (6, 10, 19, 92). While the silencing effect is pronounced in mammals, normal gene expression generally returns in 9 to 11 days (5).

The phenomenon of PTGS was first discovered in plants over a decade ago and involves specific targeting of a gene and degradation of the mRNA

resulting in a block in translation of the protein encoded by the silenced gene (1, 93). The process of PTGS is believed to have co-evolved with its viral antagonist to function as a primitive immune response against the invasion of foreign nucleic acids presented through viral infections and transposons and retroposons (3). This theory is supported by the observation that certain viruses are able to overcome or prevent mRNA degradation by expressing proteins that suppress PTGS (5). Most plant viruses possess single-stranded RNA genomes, which are replicated by the virus-encoded RNA-dependent RNA polymerase to produce both sense and antisense strands of RNA (19). These strands have the potential to hybridize to form double-stranded RNA (10). Once dsRNA, a marker for viral infection, is detected in the cell, the process of PTGS is initiated (10).

The first proposed mechanism to explain RNAi was set forth by Bass and was based on the introduction of dsRNA directly into cells to be degraded and used in gene silencing (94). Bass proposed that the dsRNA introduced into the cell is, in turn, targeted by an endonuclease which then cleaves it to short, ~23nt, dsRNA, also referred to as short interfering RNA (siRNA), which bind to and promote degradation of the free mRNA (94). This endonuclease, later termed the Dicer enzyme, is a member of the Argonaute protein family (95). It is an initiator of the formation of a 3-protein complex known as the RNA-induced silencing complex (RISC) with the siRNA for mRNA degradation (95).

The first animal application for this technique came in *Caenorhabditis elegans* where it was discovered that, as in the plant system, gene down-regulation could be heritable due to the presence of the enzyme, RNA-dependent

12

RNA polymerase (RdRp) (2, 96). The plant and *C. elegans* mechanism are similar in that dsRNA has catalytic silencing capabilities, while single stranded RNA gets degraded upon delivery into the cell (2). The mechanism by which plants and nematodes undergo gene silencing has been referred to as the "guide- primer" model, (Figure 4) where the Dicer enzyme cleaves double-stranded RNA to make short interfering (siRNA) (92). The Dicer enzyme unwinds the siRNA, and the antisense strand of the siRNA duplex binds to the homologous region of mRNA (92). These siRNAs serve as a guide-primer with RdRp to convert the mRNA into double stranded RNA to be digested by the Dicer enzyme (92). This process is propagated indefinitely due to the recycling of the template siRNA and the stability of both the RdRp and Dicer enzymes (92). The assertion that siRNAs are catalytic in nature is supported by the requirement of only a few siRNA molecules to mount a sufficient RNAi response (6, 97).

The mammalian model for gene silencing has been termed the "endonucleocytic-cleavage" model (Figure 5), which involves a group of proteins known as the RNA-induced silencing complex (RISC) (2, 92, 93, 98). The proteins included in the mammalian RISC are EIF2C2, Gemin3 and Gemin4, and an endonuclease, Slicer, activated by a helicase domain located on the Dicer enzyme (95, 98). This activation results in the unwinding of the double-stranded siRNA, leaving the antisense strand of RNA bound to the activated RISC complex (92). This siRNA serves as a template for sequence-specific targeted degradation of mRNA (92, 94). The "endonucleocytic cleavage" model proposes that the activated RISC complex binds the single-stranded mRNA template to be

13
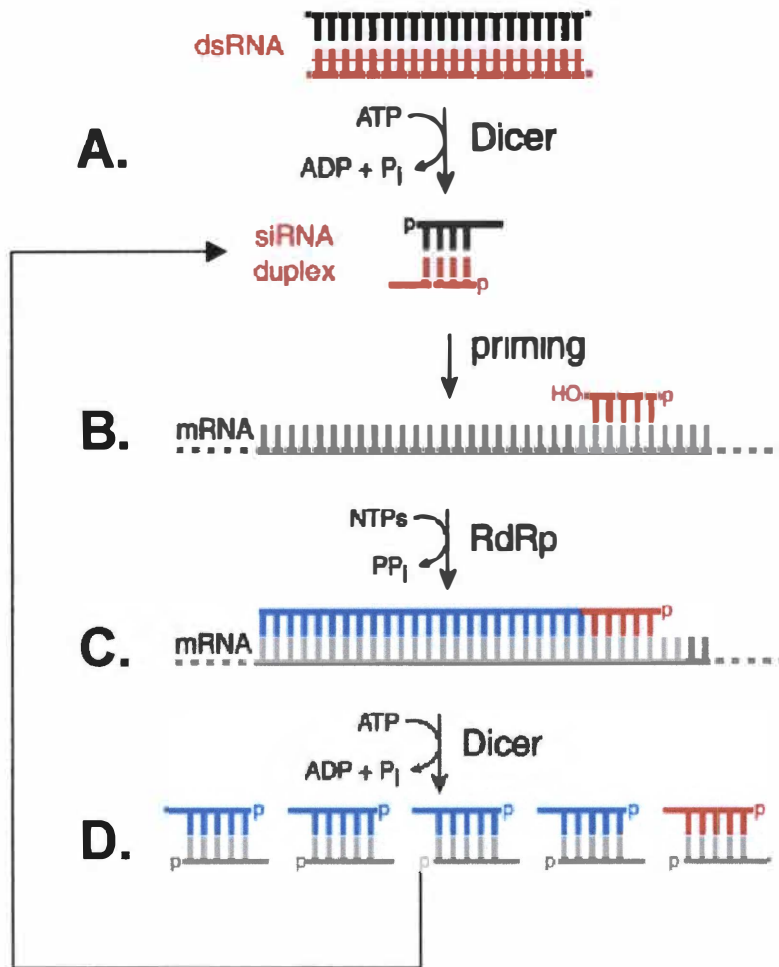
Figure 4. The "guide-primer" model. The guide-primer mechanism for gene silencing begins with the cleavage of double-stranded RNA into siRNA by the Dicer enzyme, **Panel A**, followed by the unwinding of the siRNA duplex by a helicase domain in Dicer. The antisense strand of the siRNA duplex then binds to the mRNA in a sequence-specific manner, **Panel B**. The binding of the siRNA initiates the RNA-dependent RNA polymerase **(Panel C)**, which generates double-stranded RNA to be cleaved by Dicer, **Panel D**. This process is propagated through the generation of more siRNA and continues unabated until the specific mRNA has been degraded. Adapted from Schwarz *et al.* (92).
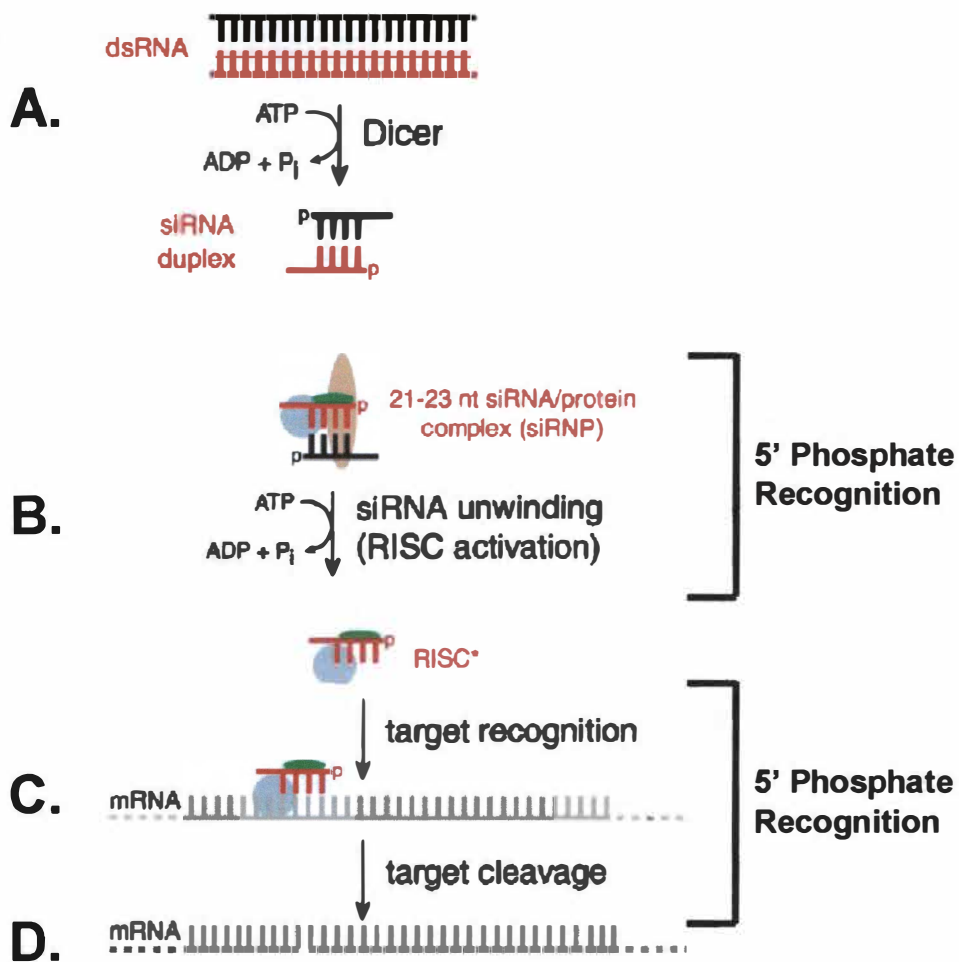
Figure 5. The "endonucleocytic-cleavage" model. The *D. melanogaster* and mammalian model for gene silencing is referred to as the "endonucleocytic-cleavage" model. The "endonucleocytic cleavage" model of gene silencing involves the RISC complex forming with the siRNA duplex. Double-stranded RNA is digested with Dicer, **Panel A.** The siRNA duplex is unwound by a helicase in the Dicer enzyme and activates the RISC complex, **Panel B.** The activated RISC binds mRNA in a sequence-specific manner **(Panel C)** and is cleaved by an endonuclease in the activated RISC complex. Adapted from Scwartz *et al.* (92).

cleaved and regenerates the Slicer endonuclease with its siRNA (Figure 5) (92, 94, 99). This process continues unabated until the mRNA has been degraded (92). The protein-endonuclease/siRNA complex co-purifies, indicating the stability of the complex (98).

The length of the dsRNA is integral to the RNAi response initiated by the cell (4, 100, 101). In an experiment designed to test the relevance of dsRNA length, Elbashir *et al* co-transfected a number of different cell lines with a luciferase-reporter plasmid and 0.21µg of siRNA or a longer dsRNA duplex (4). They observed siRNA specifically targeted the luciferase reporter gene, while the longer dsRNA duplexes strongly and nonspecifically reduced the reporter gene expression (4). The nonspecific reduction of reporter gene expression was attributed to an interferon response mounted by the cell against the dsRNA (4, 100, 101). The length dependence of 21-23 mer formation is thought to be a mechanism to prevent the undesired activation of RNAi by intramolecular base paired, non-pathogenic RNA structures (5). The location of the siRNA sequence homology is imperative for the success of the silencing effect and a single base pair mismatch can result in up to a 10% difference in efficacy (29, 102-104).

The range of RNAi applications for cancer include drug discovery, treatment, abolishing drug resistance, and cell cycle regulation (105-110). Similarly, RNAi has been explored both in CML and in Ph-positive cell lines in an attempt to silence the *Bcr-Abl* oncogene (25, 26, 28, 29, 31, 111-113). Since normal cells lack the *Bcr-Abl* fusion gene, it provides a prime molecular target for RNA interference (25, 26, 28, 29, 105, 106, 114, 115). The efficacy of targeting

16

this translocation has proven successful in a number of RNAi studies and this treatment has been effectively applied in both peripheral blood CML cells *in vitro* and a number of Ph-positive cell lines, including the K-562 cell line (28, 29, 113, 114). The long half-life of the Bcr-Abl protein, which is greater than 48 hours, has posed a problem in molecular therapies that target the Bcr-Abl gene (15, 117). This problem has been overcome using various methods designed to sustain the antisense or siRNA within the cell longer than 48 hours (30, 118).

Apoptosis

Apoptosis (programmed cell death) is the result of a sequence of events leading to the suicide of a cell (Figure 6) (119). Its function is vital to an organism and is essential in normal cell turnover, development of the immune system, embryonic development, metamorphosis, and hormone-dependent atrophy (120). The apoptotic mechanism of death occurs in two distinct phases: a commitment to cell death, followed by an execution phase, where standard morphological and biochemical changes occur (120). Some of the standard characteristics of apoptotic cell death are condensation and fragmentation of the nuclear chromatin, compaction of the cytoplasmic organelles, dilation of the endoplasmic reticulum, decreasing cell volume, and alterations to the cell membrane resulting in the recognition and phagocytosis of apoptotic cells, which prevents an inflammatory response (120). The apoptotic process can be initiated by a variety of cellular insults including DNA damage, and cytotoxicity (121). It can also be induced in the cell by intracellular factors such as the up-regulation
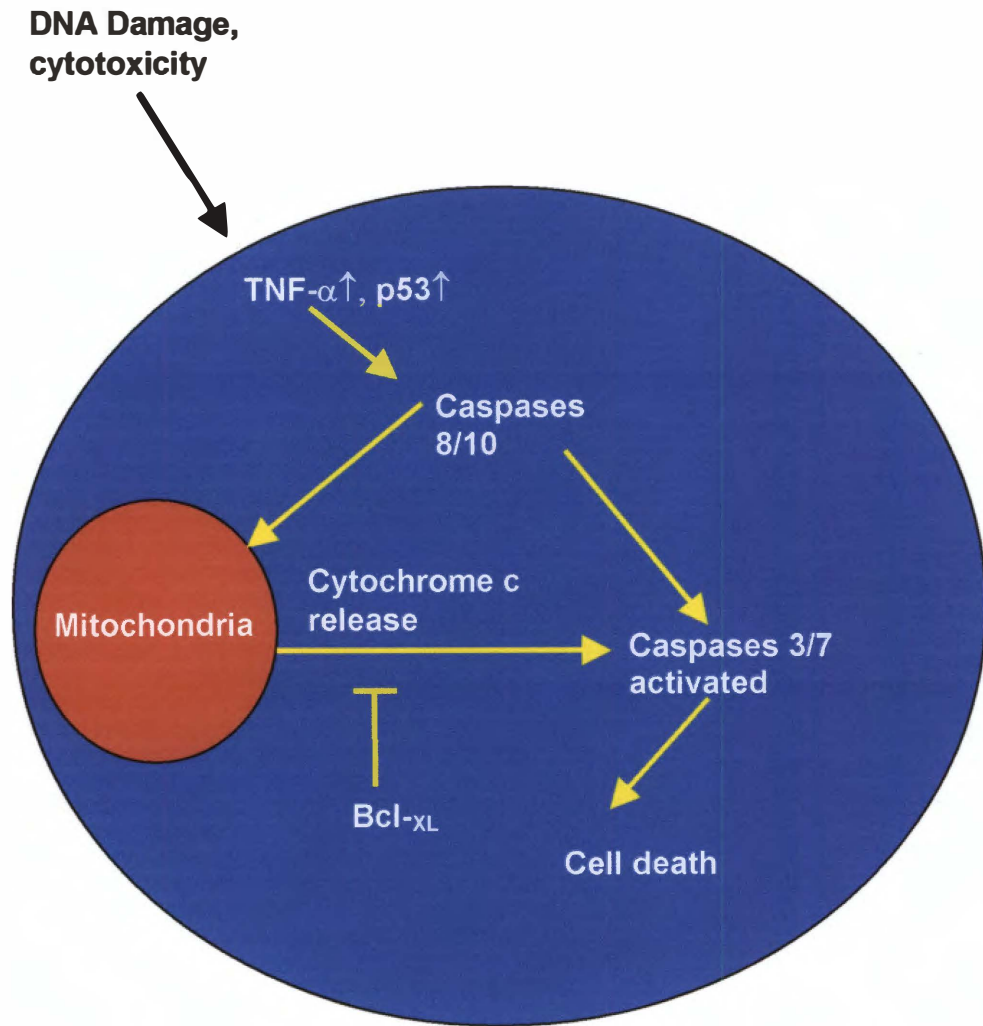
Figure 6. Apoptotic pathway. Overview of apoptotic pathway shows DNA damage and cytotoxic agents leading to activation of caspases 8 and 10. This triggers the mitochondrial membrane potential collapse to release cytochrome c, which is inhibited by Bcl-$_{XL}$. Cytochrome c results in activation of caspases 3 and 7 and leads to cell death.

of either tumor necrosis factor or p53 (122). The consequence of the apoptosis pathway is the death of a cell without an inflammatory response (119). The apoptosis cascade consists of a variety of proteins, such as caspases, and members of the Bcl-2 protein family (120, 123). To date, mammalian cells have been reported to have 12 caspases present in the zymogen, the inactive form, to prevent accidental cell death (124). Caspases are present in three types: the initiators, the executioners, and the inflammatory caspases (124). The initiators, caspases 2, 8, 9 and 10, begin the death cascade, where, through a system of biochemical signals originating from either extracellular or intracellular environment, the executioner caspases, 3, 6, 7, are activated (124).

The sequence of events during apoptosis begins with the death signal, from either the extracellular environment, or the intracellular matrix (124). The membrane proteins TRAIL, TNF-R1, Fas, or Perforin can all receive and transmit this death signal (125). Caspases 2, 8, and 10 are then activated and proceed to initiate the collapse of the mitochondrial membrane (120). The collapse of the mitochondrial membrane leads to the release of cytochrome c into the cytosol (126). The activity of caspases 3 and 7 is promoted by the presence of cytochrome c in the cytosol (126). Caspase 3 is the primary executioner caspase and has been shown to cleave and activate the DNA fragmentation factor (DFF), resulting in the DNA fragmentation step in apoptosis (126). Proteins that function in promoting apoptosis are Bax, Bak, Bad, and Bcl_{-XS}, among others (127). Proteins that serve to inhibit this process include Bcl_{-2}, Bcl_{-XL}, and Akt, among others (126, 127).

It has been discovered that Bcr-Abl serves as a negative regulator of a number of apoptotic pathways (51). One pathway for this regulation is through the inhibition of the release of mitochondrial cytochrome c and other pre-apoptotic mitochondrial events (126). This interference results in caspase 3 remaining inactive and the inhibition of apoptosis (126). Protection from apoptosis is achieved through Bcr-Abl initiating two mechanisms: constitutive activation of STAT5, and suppression of SHIP1 expression, resulting in elevated levels of phosphatidylinositol (3,4,5)-triphosphate (24). Constitutive activation of STAT5 subsequentially leads to the upregulation of the antiapoptotic protein Bcl-$_{XL}$ (39, 128, 129). Bcl-$_{XL}$ prevents perforation of the mitochondrial membrane, by functioning as an antagonist of the Bax-Bak heterodimer (124). This inhibition of Bax-Bak prevents the release of cytochrome c and other apoptotic promoters (124). The Bcl-$_{XL}$/Bax-Bak interaction is corroborated by the inhibition of Bcr-Abl resulting in the down regulation of Bcl-$_{XL}$ (39, 72). This down-regulation induces cell differentiation and leads to apoptosis through a number of death-inducing agents (126, 129-133). The proposed interaction of Bcr-Abl with STAT5, involves the Tyr[177] residue of Bcr-Abl, which shares homology with the tyrosine phosphorylation site of STAT5 (128). Down-regulation of STAT5 abrogates Bcr-Abl-dependent protection from apoptosis and leukemogenesis (128).

Based on this review of the literature it was hypothesized that targeting both the Bcr-Abl oncogene and protein using RNA interference and Gleevec in the K-562 cell line would result in restoration of apoptosis sensitivity.

Chapter 2

Materials and Methods

Cell Culture

K-562 cells, subline F_1, were passaged weekly in Eagle's minimal essential medium supplemented with 15% fetal bovine serum (FBS) (GIBCO BRL, Grand Island, NY), plus nonessential amino acids with an inoculum of 1.5 x 10^4 cells/ml (134). The cultures were incubated at 37°C in 5% CO_2. K-562 cells from 10 ml cultures were pelleted, the supernatants removed, and the pellets resuspended in 10 ml RPMI 1640 medium supplemented with L-glutamine, 10% FBS, and Gentamicin (800μg/ml) (Sigma, St. Louis, MO) at 37°C in 5% CO_2.

Proliferation

MTT assay

Mitochondrial function was assayed colorimetrically through the conversion of the substrate, MTT (3-[4,5-Dimethylthiazol-2-yl]-2,5-diphenyl-tetrazolium bromide) (Sigma, St. Louis, MO). Reactions, 0.5ml, were performed in 24-well plate where K-562 cells (subline F_1) were incubated with at 37°C with 5% CO_2 for two hours in the presence of 500μg/ml MTT. The cells were centrifuged at 14,000 x g for 5 minutes and the supernatant removed. The cells were lysed by vortexing in 700μl 2-propanol for 5 minutes. Equal aliquots were

assayed in quadruplicate on a 96-well plate with a propanol blank read by an EL340 microplate reader (Biotek, Winooski, VT) at a wavelength of 570nm with a background subtraction of 630-690nm (135).

[^{3}H]-thymidine incorporation assay

Incorporation of tritiated thymidine ([^{3}H]-thymidine) (ICN, Newport Beach, CA) was assayed using 0.25µCi in 50µl complete RPMI 1640 media. 100µl K-562 cells (subline F$_1$) suspended in complete RPMI 1640 media were co-cultured with 50µl tritiated thymidine in quadruplicate for 4 hours at 37°C with 5% CO_2. The cells were harvested with a cell harvester (Skatron Instruments, Inc., Sterling, VA) and radioactivity was assayed at counts per minute (cpm) in a Packard (Downer's Grove, IL) liquid scintillation analyzer (136).

Apoptosis

Mitochondrial Membrane Potential Assay

To measure apoptosis, two different methods were used: 1) measurement of loss of the mitochondrial membrane potential (137) 2) measurement of the activity of the caspase 3 enzyme (138). The JC-1 bi-fluorescent dye was used to measure apoptosis by flow cytometry. The green, monomeric dye is absorbed into the mitochondria in healthy cells and reaches a critical concentration where it then aggregates and emits red light. The loss of the red signal is the measure of apoptosis. K-562 cells were pelleted at 2200 x g for 10 minutes and the supernatant removed. The cells were then resuspended in 1ml PBS, [137mM

22

NaCl, 2.7mM KCl, 10mM Na-PO$_4$, pH 7.4] (InnoGenex, San Ramon, CA) in the presence of 5µg/ml JC-1 bi-fluorescent dye (Molecular Probes, Eugene, OR) with vigorous pipetting and incubated on a rocker at 37°C with 5% CO$_2$ for 20 minutes. The cells were centrifuged at 2000 x g for 5 minutes and the supernatant removed. Cells were washed twice with 1ml of PBS and centrifuged at 2000 x g for 5 minutes and the supernatant removed. The cells were resuspended in 500µl PBS and a total of 10,000 events were assayed using flow cytometry. As cells progressed into apoptosis, the early depolarization of the mitochondria was a reliable qualitative method for identifying programmed cell death (137).

Caspase 3 Assay

To measure caspase 3 activity, K-562 cells were pelleted at 2200 x g for 10 minutes and lysed with 100µl lysis buffer (Chemicon, Temecula, CA). 20µl total protein lysate was then incubated with caspase 3 substrate (ac-DEVD-pNA) (Oncogene, La Jolla, CA) in quadruplicate on a 96 well plate for 6 hours. The caspase 3 activity was measured at a wavelength of 405nm on an EL340 microplate reader (Biotek). As the cells underwent apoptosis, the caspase 3 activity increased (138).

<u>Cloning</u>

siRNA synthesis for RNAi involves cloning, isolation and amplification of the region of interest, and the subsequent processing of this region into siRNA.

This site-specific siRNA is then inserted into the cell through transfection using cationic liposomes and the silencing effect is then assayed through various methods including protein quantification, and mRNA degradation. To generate siRNA, the *Bcr-Abl* fragment was first cloned into the Litmus 28 plasmid vector (New England Biolabs, Beverly, MA).

Primer Design

Primers specific for Bcr-Abl oncogene were designed according to sequence data from the NCBI BLAST database. The sequences used in the design of *Bcr-Abl* specific primers were identified by accession numbers Y00661 (Human bcr mRNA) and X16416 (Human c-abl mRNA). The Bcr-Abl forward (SS) strand primer begins at base 3166 with the break point located 212 bp downstream at base 3378. The Bcr-Abl reverse (AS) strand primer begins at base 468 with the breakpoint located 241 bp upstream at base 227. The resultant PCR product is 453 bp long with the fusion site located approximately in the center of the strand. PCR primers were also designed to flank the T7/polylinker region for verification of positive colonies. Primers were made by Sigma Genosys (Midland, TX).

Bcr-Abl Primer Sequence

Forward (SS): 5'-ggagggagaacatccgggagcagc-3' – position (3166-3190)

Reverse (AS): 5'-gccattttttggtttgggcttcacag-3' – position (468-443)

RNA isolation

K-562 cells were centrifuged at 2200 x g for 10 minutes and the media was removed. The cells were then lysed with 1ml TRIzol (Invitrogen, Carlsbad, CA) transferred to 1.5ml sterile tubes and 200µl chloroform was added (139). The Chloroform/TRIzol cell lysate was vortexed and then centrifuged at 12,000 x g for 5 minutes. The upper aqueous phase was then removed and transferred to a new tube and an equal volume of acidic (pH 4.6) phenol/chloroform (1:1) was added. The tubes were shaken and centrifuged at 12,000 x g for 5 minutes and the upper layer was transferred to a new tube. The phenol/chloroform extraction was repeated two times. Sodium acetate, pH 5.2, (1:10 volume), 100% ethanol (two volumes), and 10µl (5mg/ml) linear acrylamide carrier (Ambion, Austin, TX) was added and incubated at -80°C for 1 hour. RNA was centrifuged at 14,000 x g for 10 minutes and the supernatant removed. The pellet was washed with 80% ethanol twice, air-dried for 5 minutes, and resuspended in nuclease-free water. For storage, 1.5µl RNAse antibody (1:20 volume) was added to prevent degradation during storage. RNA was quantified on a UV spectrophotometer at 260nm and quantified using the Beer-Lambert law, O.D./260 x 40µg/ml x dilution factor = RNA concentration in µg/ml.

Reverse Transcription-Polymerase Chain Reaction (RT-PCR)

Once the total RNA was purified, the mRNA served as a template in the RT-PCR reaction to generate cDNA. 1.5µl (2µg/µl) RNA was added to 2.5ng/µl random hexamer, 1µM *Bcr-Abl* reverse antisense primer, 1.5µl nuclease-free

water to a total volume of 4µl. The reaction mixture was placed on a heating block pre-warmed to 65°C for 2 minutes, then placed on ice. In a separate tube, reverse transcriptase, thermoscript (0.75 units/µl), superscript II (10 units/µl), and superscript III (10 units/µl) were used, and RNAse- out (2 units/µl) was added to 5µl 2X reaction buffer to a total volume of 6µl (Invitrogen, Carlsbad, CA). The reaction mix was combined with the RNA/primer mix to create a total reaction volume of 10µl. The reaction was incubated at 25°C for ten minutes to allow for primer hybridization, and then transferred to a water bath at 56°C for 90 minutes.

Polymerase Chain Reaction (PCR)

The cDNA generated from the RT-PCR was subjected to *Bcr-Abl* gene-specific primer amplification through PCR. The initial reactions were done in 16µl total volume and later reactions were scaled up to 50µl. For the 16µl reaction, 8µl 2X PCR Buffer with Enhance component (1ml buffer mix = 200µl 10X PCR Buffer, 400µl 5X Enhance, 40µl 10mM dNTP mix, 360µl nuclease-free water), Taq DNA Polymerase (0.02 units/µl) (Eppendorf, Westbury, NY), 4µl cDNA template, 1.25µM *Bcr-Abl* forward (SS) and reverse (AS) primers, 2µl nuclease-free water. The reaction conditions were as follows: 97°C initial denaturation for 2 minutes followed by 35 cycles at 94°C for 1 minute, 55°C for 1 minute, 72°C for 2 minutes and ended with an extension at 72°C for 7 minutes. The samples were then held at 4°C, analyzed on an agarose gel and stored at -20°C for later usage.

26

Real Time PCR

The real time reactions using the QuantiTect gene expression assay system (Qiagen, Gaithersburg, MD) were assembled in triplicate as follows: master mix [12.5 µl 2X QuantiTect probe RT-PCR master mix, 2.5 µl 10X QuantiTect assay mix (probes were specific for *Bcr-Abl* and *GAPDH*), 0.25 µl QuantiTect RT mix, 4.75 µl RNAse free water] and 5 µl template RNA (diluted 1:50 and 1:100) to a total reaction volume of 25 µl. The cycle parameters were: reverse transcription for 30 minutes at 50°C; PCR initial activation step of 95°C for 15 minutes; 3 step cycling: denaturation 15 s at 94°C, annealing/detection 30 s at 56°C, extension 30 s at 76°C; cycles were repeated for 45 cycles. Standards were made for both *Bcr-Abl* and for *GAPDH* through a series of dilutions of RNA to concentrations of 250ng/5µl, 100ng/5µl, 25ng/5µl, 10ng/5µl, 1ng/5µl. These standards were used to quantify the levels of *Bcr-Abl* and *GAPDH* expression of the experimental groups.

EcoRV Digestion

To prepare the Litmus 28i vector (New England Biolabs, Beverly, MA) for cloning, the vector was digested with EcoRV at a site in the polylinker located between two opposing T7 promoters. The digestion protocol was as follows: EcoRV (1 units/µl, Promega, Madison, WI), BSA (0.001µg/µl, Promega), 4µl NEB Buffer 3 (New England Biolabs), Litmus 28i plasmid vector (25ng/µl, New England Biolabs), 29.6µl molecular grade water to a total reaction volume of

40µl. The digestion mixture was incubated at 37°C for 2 hours, followed by incubation at 25°C for 2 hours, and a final heat inactivation at 80°C for 20 minutes. The linearized vector was confirmed on a 1% agarose gel and then stored at -20°C for later usage. This digestion yielded a blunt, linearized vector suitable for cloning.

Klenow Fragment/T4 Polynucleotide Kinase Reaction

To prepare the Bcr-Abl oncogene fragment for cloning into the Litmus 28i plasmid vector, the fragment was digested with Klenow fragment for blunt end polishing. The digestion protocol was as follows: Bcr-Abl fragment (37.2ng/µl), 10µl 2X Quick Ligation Buffer (New England Biolabs), dNTP (465µM, Eppendorf), Klenow fragment (0.0465 units/µl, New England Biolabs) to a total reaction volume of 21.5µl. The Klenow reaction was incubated at 25°C for 15 minutes and then heat killed at 75°C for 20 minutes. This reaction was supplemented with 850µM ATP and T4 polynucleotide kinase (0.4 units/µl, New England Biolabs) and incubated at 37°C for 30 minutes. The T4 polynucleotide kinase reaction was then heat inactivated at 65°C for 20 minutes. The final concentration of the modified *Bcr-Abl* oncogene fragment was determined to be 40ng/µl on a 2% agarose gel.

Ligation of *Bcr-Abl* into Litmus 28i Plasmid Vector

Ligation reactions were assembled in two different reactions of vector:insert ratios, 1:3 and 1:4. The 1:3 vector:insert reaction was as follows: Litmus 28i plasmid vector (20ng/µl), *Bcr-Abl* (10ng/µl) oncogene fragment insert, Quick DNA Ligase (0.2 units/µl, New England Biolabs), and 2X Quick Ligation Buffer (New England Biolabs) to a total volume of 5.5µl. The 1:4 vector:insert reaction was as follows: Litmus 28i plasmid vector (18.5ng/µl), Bcr-Abl oncogene fragment insert (12.5ng/µl), Quick DNA Ligase (0.15 units/µl, New England Biolabs), and 2X Quick Ligation Buffer (New England Biolabs) to a total volume of 6.5µl. To verify the presence of Bcr-Abl insert-positive Litmus 28i plasmids, the ligation reaction was digested with EcoRV to eliminate the background and then subjected to PCR with the Litmus 28i specific primers flanking the site of insertion into the vector.

Transformation of Ligation into Competent *E. coli* Cells

In a sterile 5ml tube, 2.5µl of the ligation reaction digested with EcoRV was incubated with 25µl Nova Blue competent cells (Novagen, Madison, WI) on ice for 30 minutes. The cell/ligation mix was then heat shocked at 42°C for 1minute and then placed on ice for 2 minutes. 150µl of prewarmed SOC media was added to the cell/ligation mix and incubated at 37°C, shaking at 225rpm for 1 hour. The cells were then plated onto prewarmed LB agar plates with 100µg/ml Carbenicillin (Invitrogen), and incubated at 37°C overnight. Five colonies were selected and tested through PCR amplification with the Litmus primers. Positive

colonies were grown overnight, plasmid preps were made for siRNA generation and glycerol stocks were prepared and stored at -80°C. These positive clones were sequenced to verify accuracy of the sequence as compared to the published BLAST data.

RNAi

siRNA Generation

Double-stranded DNA was obtained through the PCR of the Litmus 28i/Bcr-Abl as well as the Litmus 28i/LitMal insert with T7 primers under these conditions: 97°C initial denaturation for 2 minutes followed by 35 cycles at 94°C for 1 minute, 55°C for 1 minute, 72°C for 2 minutes and ended with an extension at 72°C for 7 minutes, holding at 4°C. DNA was then subjected to T7 RNA Polymerase amplification to generate double stranded RNA. The reaction protocol was as follows: template DNA (100ng/μl), 2μl 10X Reaction Buffer, 8μl NTP mix, 2μl T7 RNA Polymerase (Ambion), and nuclease-free water to a total reaction volume of 20μl. The reaction was incubated at 37°C for 2 hours followed by a digestion with DNAse 1 and RNAse A to eliminate the DNA template and single stranded RNA. The digestion protocol is as follows: 20μl T7 RNA Polymerase reaction, 21μl nuclease free water, 5μl 10X Digestion Buffer, DNAse 1 (0.8 units/μl), and RNAse A (40pg/μl) to a total reaction volume of 50μl, was incubated at 37°C for 1 hour. The product was column purified, quantified with A_{260} and analyzed on a 1.5% agarose gel. The final step in generating the siRNA involved the digestion of the double-stranded RNA with RNAse III as follows:

30

dsRNA (300ng/µl), 5µl 10X RNAse III Buffer, RNAse III (0.3 units/µl, Ambion), and nuclease-free water to a total reaction volume of 50µl. The RNAse III digestion reaction was incubated at 37°C for 1 hour and the siRNA were column purified and quantified with A_{260} and analyzed on a 12% polyacrylamide gel.

Transfection

Transfection was carried out with varying molar concentrations of siRNA with a set amount of RNAifect (Qiagen). Transfection protocol was as follows: in a sterile PCR tube siRNA was diluted in RPMI 1640 media, 10% serum (Atlanta Biologicals) with gentamicin to a total volume of 100µl. RNAifect, 10µg/ml, at a ratio of 6µl:1µg siRNA was added to 100µl siRNA mix and incubated at room temperature for 25 minutes to allow for complex formation. After formation, the complex was then added to the K-562 cells suspended in 100µl RPMI 1640 media, 10% FBS, with gentamicin in a 24-well plate in a total transfection volume of 200µl to transfect for 4 -10 hours at 37°C with 5% CO_2. Upon completion of the transfection, the cells were then added to 10ml flasks with RPMI 1640 media, with 10% FBS and Gentamicin (80µg/ml) and grown for the duration of the experiment at 37°C with 5% CO_2.

Western Blot

K-562 cells were pelleted at 2,200 x g for 5 minutes and the supernatant removed. The cells were lysed in Chaps Cell Extract Buffer [50mM Pipes/NaOH

(pH 6.5), 2mM EDTA, 0.1% Chaps, 5mM DTT, 20 µg/ml Leupeptin, 10 µg/ml pepstatin, 10 µg/ml aprotinin, and 1mM PMSF] for 30 minutes on ice. The lysate was centrifuged at 14,000 rpm for 10 minutes and the supenatant transferred to a new tube. Protein concentration was quantified using Bradford analysis on an EL340 microplate reader (Biotek) and 65µg total protein used in western blot assay.

The protein was loaded into a 6% SDS denaturing gel and electrophoresed at 125V for 1½ hours. The protein was transferred onto a nitrocellulose membrane at 70V at 4°C for 1 hour. The nitrocellulose membrane was blocked using casein for 1 hour. Primary antibodies: α–rabbit Bcr (Santa Cruz Biologicals, Santa Cruz, CA), α-rabbit Bcl-$_{XL}$ (Spring Bioscience, Fremont, CA) dilutions of 1:1000 in casein, was applied on nitrocellulose membrane at 4°C overnight with shaking. The membrane was washed 3 times for 5 minutes in TBST and the secondary antibody, α–rabbit IgG conjugated with horseradish peroxidase (dilution of 1:5000 in casein), was applied to the membrane with shaking for 1 hour. The membrane was washed 5 times for 5 minutes in TBST and the substrate was applied for 5 minutes. The protein was visualized using X-ray film.

Chapter 3

Results

Gleevec

Proliferation was measured using two independent assays, MTT salt conversion, which quantified the loss of mitochondrial membrane potential, and $[^3H]$-thymidine uptake, which determined the level of DNA synthesis. Both of these proliferation studies were set up to establish the IC_{50}, where 50% viability was present, of Gleevec was established in the F_1 subline of K-562 cells. Through a series of time-course, dose response experiments performed in triplicate over the course of three weeks, the average of all the proliferation data was compiled into a dose response curve of Gleevec. From these averages the IC_{50} was determined. Time points were taken at 24, 48, 72, and 96 hours to determine the optimal time for assaying the effects of Gleevec; the data from times 24 hours and 96 hours was not included. In both the MTT and the $[^3H]$-thymidine uptake experiments, the IC_{50} of Gleevec was found to be 0.2 μM (figures 7 and 8). Both time points 48 and 72 hours were used for later studies.

The next study measured the level of apoptosis in response to the stress of Gleevec through both caspase 3 activity and loss of mitochondrial membrane potential. In this study the empirical IC_{50} found through proliferative measure was corroborated by apoptosis experiments to confirm that the decline in proliferation was, in fact, due to programmed cell death.
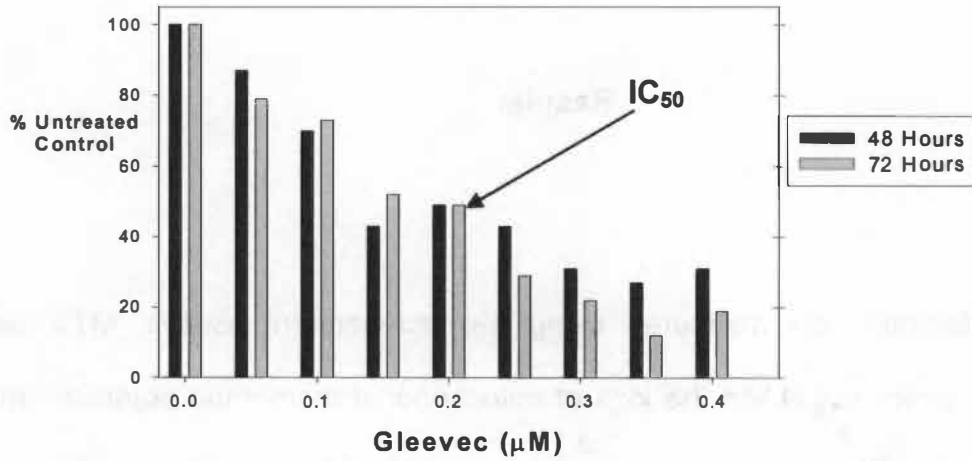
MTT Dose Response

Figure 7. The IC_{50} of Gleevec determined by MTT reduction. An average of 3 weeks data (n = 9) of the K-562 subline F_1 co-cultured with varying doses of Gleevec assayed at 48 and 72 hours indicated the IC_{50} of Gleevec to be 0.2μM.
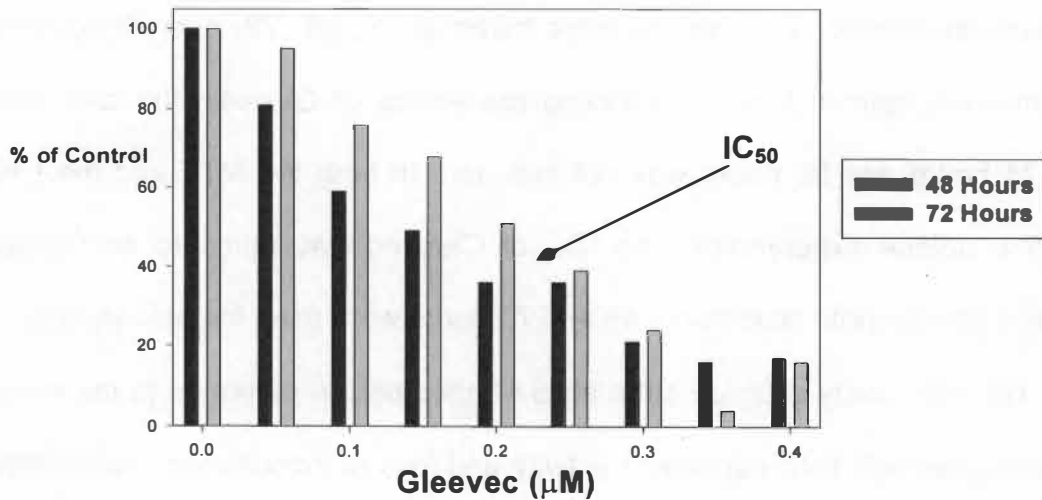
[³H]-Thymidine Uptake Dose Response

Figure 8. The IC_{50} of Gleevec determined by [³H]-thymidine uptake. An average of 3 weeks data (n = 9) of the K-562 subline F_1 co-cultured with varying doses of Gleevec assayed at 48 and 72 hours indicated the IC_{50} of Gleevec to be 0.2μM.

Caspase 3 activity is shown to be elevated as a response to increasing doses of Gleevec at 48 and 72 hours (Figures 9 and 10). There was baseline caspase 3 activity up to 0.2 μM, but doses beyond this resulted in a greater than 5-fold increase in caspase 3 activity at both 48 and 72 hours. The mitochondrial membrane integrity measured by FACS analysis is shown in response to Gleevec stress at 48 and 72 hours (Figures 11 and 12). With doses above 0.2 μM, Gleevec induces a greater than 5-fold increase in apoptotic cells at 48 hours, and a greater than 20-fold increase in apoptotic cells at 72 hours.

Proliferative decline was determined to be a result of apoptosis as [^{3}H]-thymidine data at 48 and 72 hours was co-plotted with caspase 3 data at 48 hours and 72 hours (Figures 13 and 14). This inverse relationship shows 0.2 μM Gleevec as the effective dose at both inducing apoptosis and reducing viability by 50%. These findings corroborate the previously published Gleevec IC_{50} of 0.25μM (34, 35).

RNAi

The *Bcr-Abl* fusion gene was cloned into the Lit 28 RNA transcription vector (Figure 15) used to *in vitro* transcribe double-stranded RNA for making siRNA to be used later in the study. The blunt, non-directional method of cloning was chosen because the orientation was irrelevant. The *Bcr-Abl* fusion gene product, 450bp, and the Lit28i vector was gel purified and prepared for ligation (Figure 16). To measure the success of the reaction, the ligation product was digested with EcoRV and subjected to PCR (Figure 17). This digestion limited the

Caspase 3 Activity at 48 Hours

Figure 9. Apoptosis measured by caspase 3 activity at 48 hours. Apoptosis determined by caspase 3 activity in the K-562 subline F_1 co-cultured with varying doses of Gleevec assayed at 48 hours indicated that doses greater than 0.2µM induced apoptosis.

Caspase 3 Activity at 72 Hours

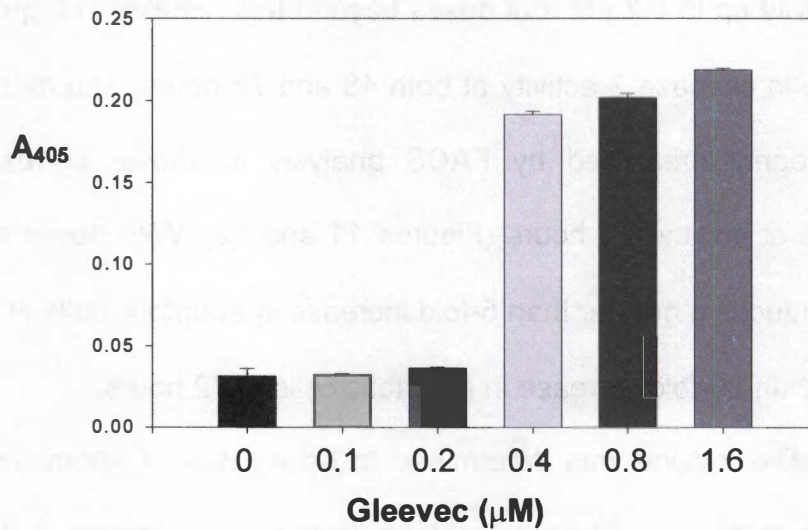**Figure 10.** Apoptosis measured by caspase 3 activity at 72 hours. Apoptosis determined by caspase 3 activity in the K-562 subline F_1 co-cultured with varying doses of Gleevec assayed at 72 hours indicated that doses greater than 0.2μM induced apoptosis.

Mitochondrial Membrane Potential at 48 hours
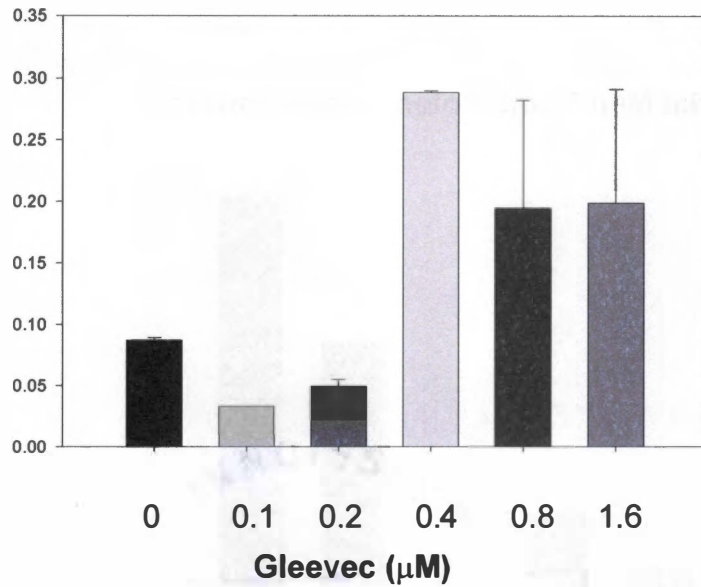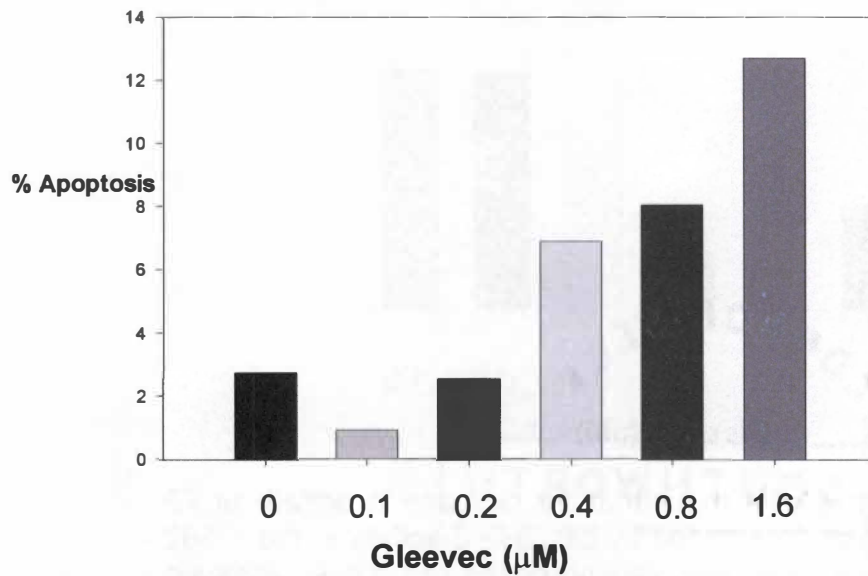

Figure 11. Mitochondrial membrane potential at 48 hours. The K-562 subline F_1 co-cultured with varying doses of Gleevec indicated that doses greater than 0.2μM induced apoptosis at 48 hours.

Mitochondrial Membrane Potential at 72 hours
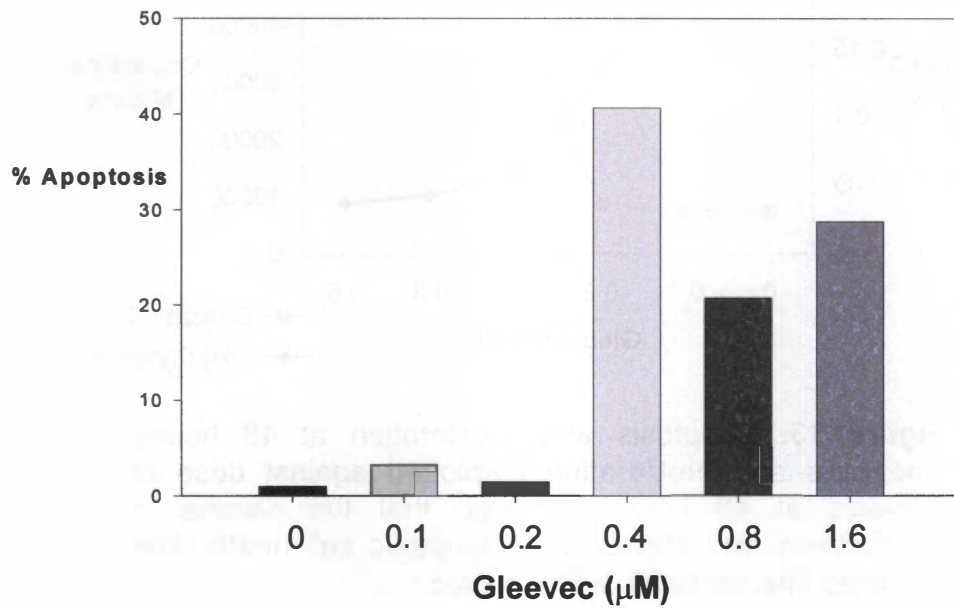
Figure 12. Mitochondrial membrane potential at 72 hours. The K-562 subline F_1 co-cultured with varying doses of Gleevec indicated that doses greater than 0.2µM induced apoptosis at 72 hours.
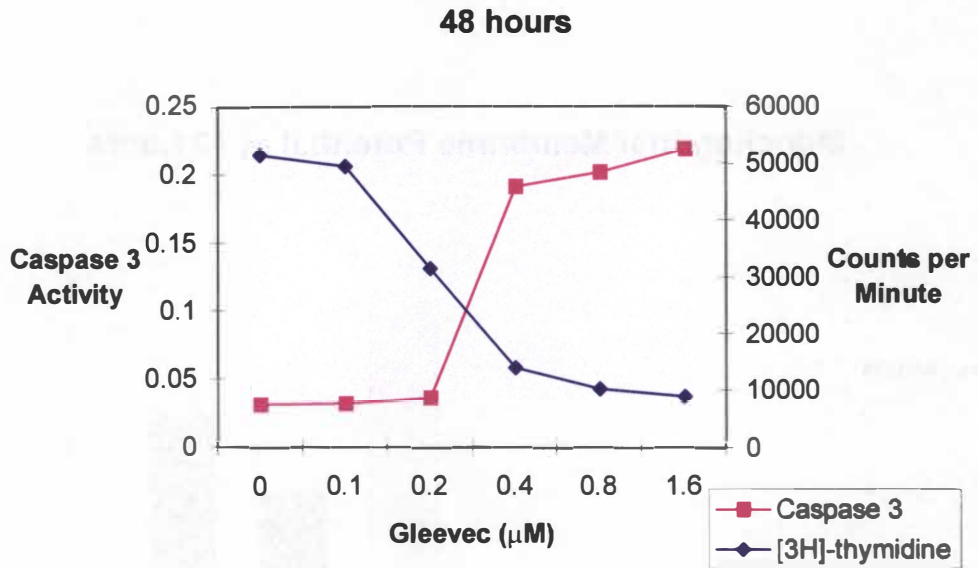
48 hours

Figure 13. Apoptosis and proliferation at 48 hours. Apoptosis and proliferation co-plotted against dose of Gleevec at 48 hours indicated that the decline in proliferation was attributed to apoptotic cell death. The two lines intersect at 0.3μM Gleevec.
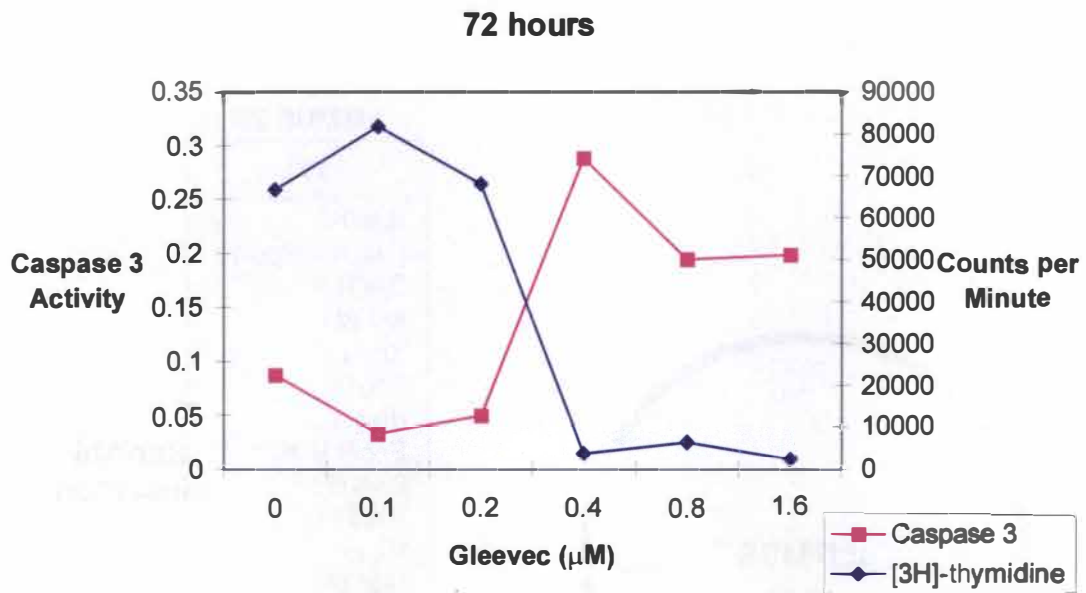
72 hours

Figure 14. Apoptosis and proliferation at 72 hours. Apoptosis and proliferation co-plotted against dose of Gleevec at 72 hours indicated that the decline in proliferation was attributed to apoptotic cell death. The lines intersect at 0.3μM Gleevec.
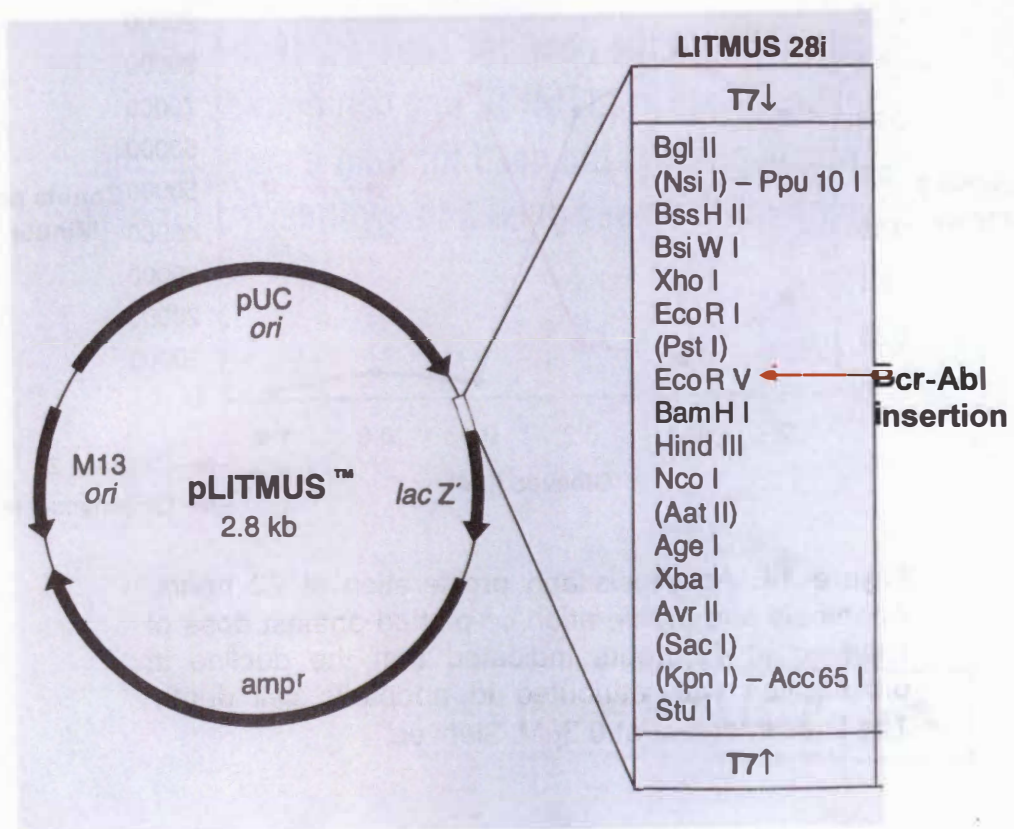
Figure 15. The Litmus 28i plasmid vector. The Litmus 28i plasmid vector used for *in vitro* production of siRNA contains two opposing T7 promoters. The *Bcr-Abl* fusion gene was cloned into the polylinker region at the blunt EcoRV site.

450bp →

1 2 3 4 5 6 7 8 9 10 11
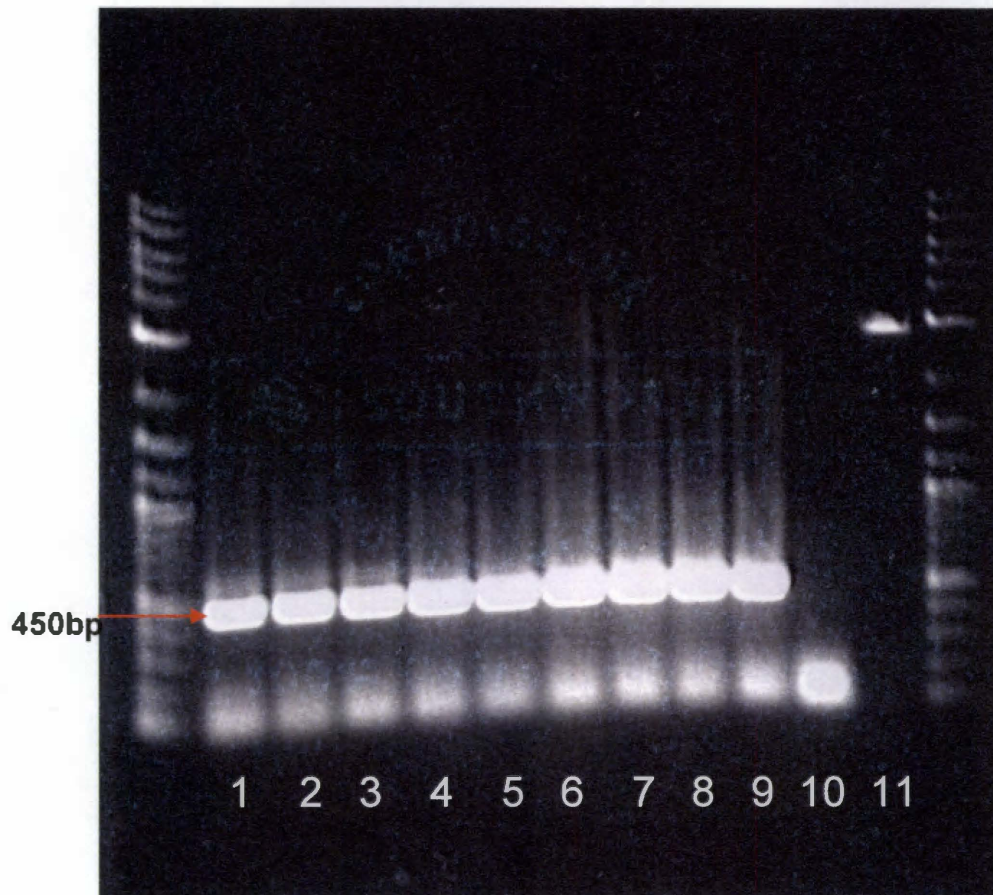
Figure 16. Purification of the Bcr-Abl PCR product for cloning.1% agarose gel stained with ethidium bromide. PCR product of BCR-ABL fragment, cut from this gel and then purified using the Wizard PCR cleanup kit (Promega). **Lanes 1-9:** BCR-ABL fragment 1 (450bp), **Lane 10:** negative control (no template), **Lane 11:** EcoRV digested Litmus 28i plasmid.
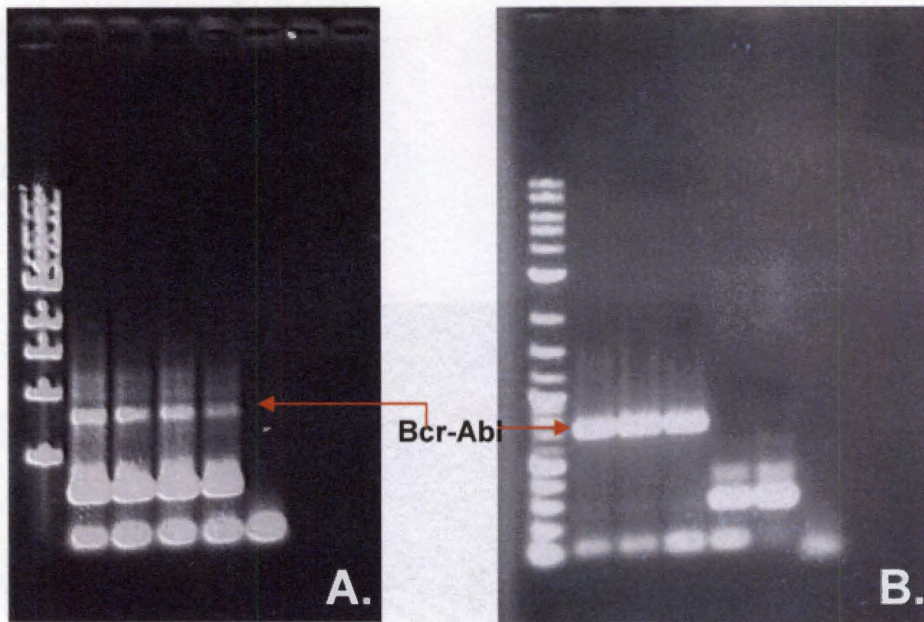
Figure 17. Confirmation of Bcr-Abl positive clones through PCR. **Panel A:** Ligation reaction was digested with EcoRV and PCR confirmed the presence of the *Bcr-Abl* insert. **Panel B:** Plasmid DNA was isolated, column purified and PCR confirmed the *Bcr-Abl* positive colonies.

background of the re-ligated vector and allowed for confirmation of the ligation for procession to the next step of transformation. Following the ligation and the transformation into competent *Escherichia coli* cells, five colonies were present. Of these five colonies, three were found to be positive for the *Bcr-Abl* insert (Figure 17). Through restriction endonuclease digestion, two of the three colonies were confirmed to be positive for the *Bcr-Abl* insert (Figure 18). This step was confirmed through additional PCR (data not included) and through sequencing (Figures 19 and 20).

Following the confirmation of the Bcr-Abl insert, the Bcr-Abl-specific siRNA were made through amplification with T7 RNA polymerase (Figure 21) and digested with RNAse III (140). This product yielded 15-19 nucleotide duplexes homologous to the 450 bp region of the Bcr-Abl insert. The integrity of these siRNA is shown in Figure 22.

Transfection at first proved to be a problem and limiting factor in the knockdown of the Bcr-Abl transcript. Transfection efficiency was measured and optimized using a non-silencing, fluorescein-labeled siRNA duplex. Oligofectamine yielded 25% transfection efficiency as measured through flow cytometry (Figure 23), and was not detectable using fluorescent microscopy. Delivery the siRNA into the K-562 cells was accomplished using RNAifect, with consistent efficiencies of 90% or better as measured through both flow cytometry (Figure 23) and fluorescent microscopy (Figure 24). RNAifect transfections were performed in complete media, whereas Oligofectamine transfections were performed in the absence of serum and were more cytotoxic.
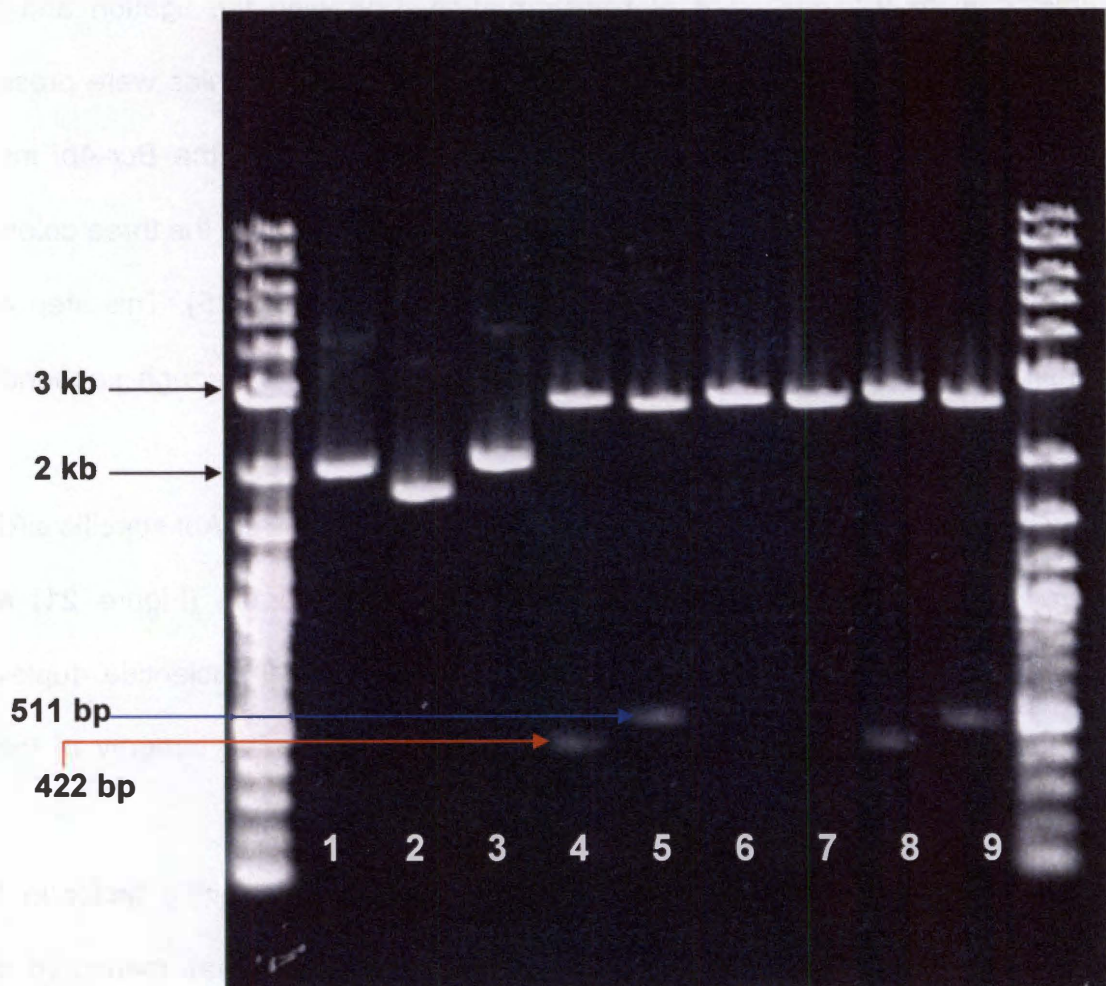
Figure 18. Restriction enzyme digestion. 1% Agarose gel stained with Ethidium Bromide. Plasmids 1, 2 and 3 were digested with Hind III to confirm orientation, and then double digested with XhoI and XbaI to confirm the size of the insert. **Lane 1:** plasmid 1 undigested, **Lane 2:** plasmid 2 undigested, **Lane 3:** plasmid 3 undigested, **Lane 4:** plasmid 1 digested with Hind III (422bp), **Lane 5:** plasmid 1 double digested with XhoI and XbaI (511bp), **Lane 6:** plasmid 2 digested with Hind III, **Lane 7:** plasmid 2 double digested with XhoI and XbaI, **Lane 8:** plasmid 3 digested with Hind III (422bp), **Lane 9:** plasmid 3 double digested with XhoI and XbaI (511bp).
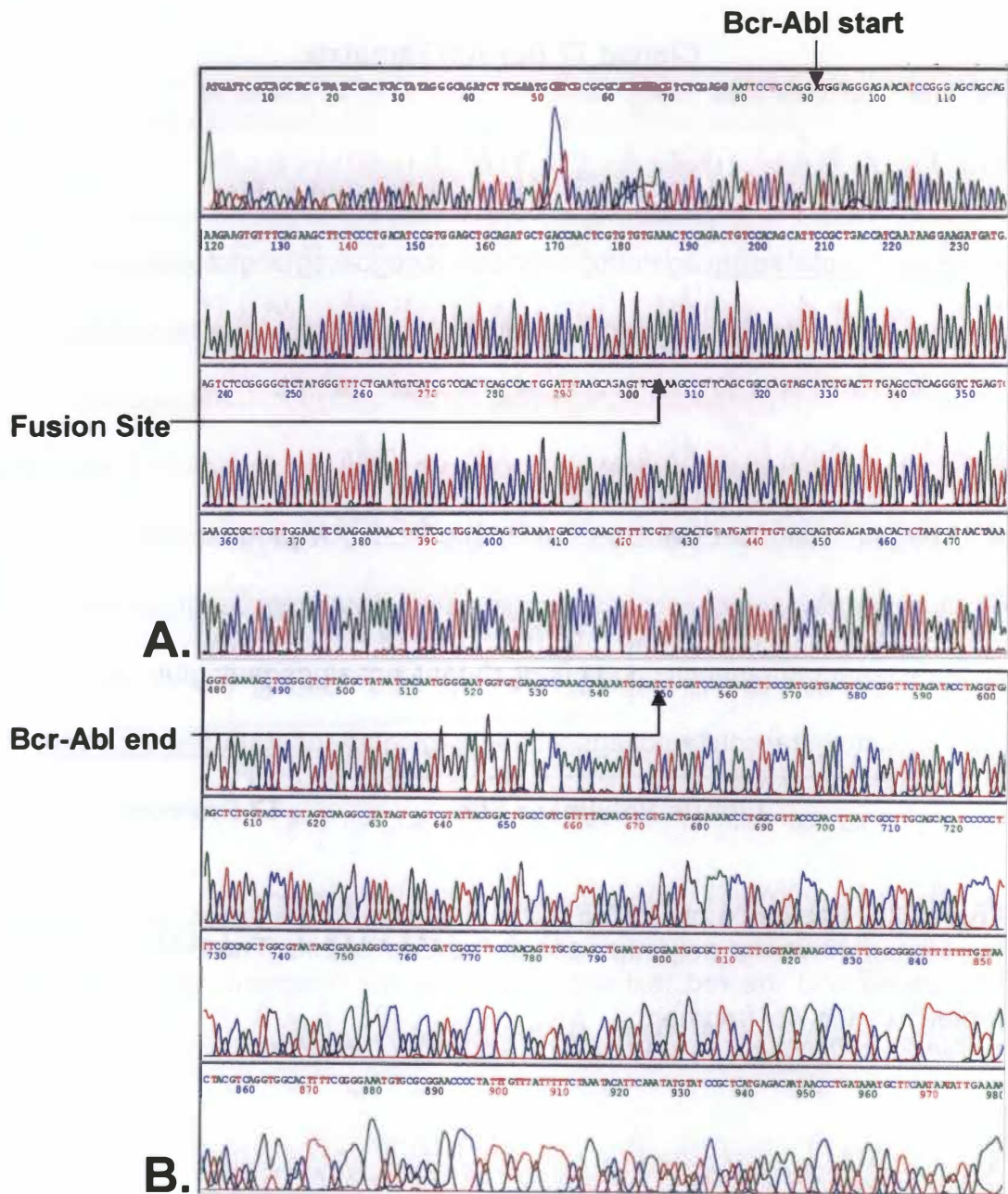
Figure 19. Sequence data of Lit28i/Bcr-Abl. Litmus sequencing primers specific for the Litmus 28 plasmid were used to sequence DNA spanning the polylinker region including the cloned Bcr-Abl insert. **Panel A:** includes the start of the Bcr-Abl oncogene as well as the fusion site **Panel B:** includes the end of the Bcr-Abl oncogene.

Cloned T7 Bcr-Abl Template

T7 promoter   **Litmus Polylinker Site**

5'**taatacgactcactataggg**cagatcttcgaatgccatcgcgcgcaccgtacgtctcgaggaattcctgcag

gggagggagaacatccgggagcagcagaagaagtgtttcagaagcttctccctgacatccgtggagctgcag

atgctgaccaactcgtgtgtgaaactccagactgtccacagcattccgctgaccatcaataaggaagatgatga

gtctccgggggctctatgggtttctgaatgtcatcgtccactcagccactggatttaagcagagttcaaaagcccttc

agcggccagtagcatctgactttgagcctcagggtctgagtgaagccgctcgttggaactccaaggaaaacctt

ctcgctggacccagtgaaaatgaccccaacctttcgttgcactgtatgatttgtggccagtggagataacactct

aagcataactaaaggtgaaaagctccgggtcttaggctataatcacaatggggaatggtgtgaagcccaaacc

aaaaatggc gctctggtaccctctagtcaaggccttaagtgagtcgtatta**ccctatagtgagtcgtatta** ³'

Litmus Polylinker Site   **T7 Promoter**

Figure 20. Sequence of Lit28i/Bcr-Abl. The *Bcr-Abl* fragment was cloned into the Litmus 28 vector polylinker site at the EcoRV site. The *Bcr-Abl* gene was sequenced and the red text represents the *Bcr* fragment, and the blue text represents the *Abl* fragment.
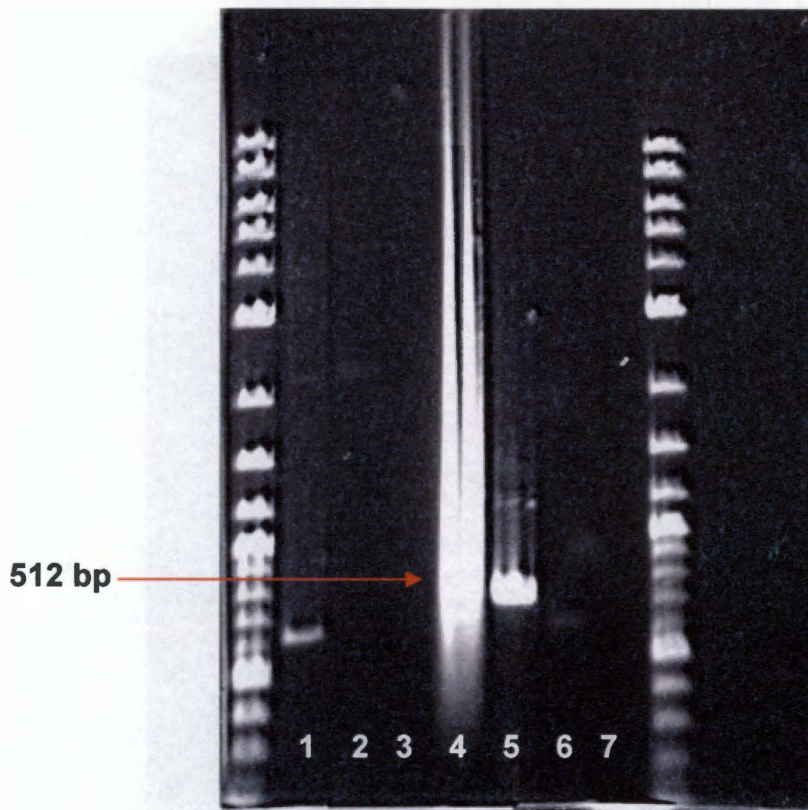
512 bp ⟶

Figure 21. Two different preparations of double-stranded RNA. 1% agarose gel stained with ethidium bromide. Double stranded DNA and double stranded RNA generated through PCR and RT-PCR respectively. **Lane 1:** PCR DNA product (512bp), **Lane 2:** Negative control (no primers), **Lane 3:** Negative control (no template), **Lane 4:** dsRNA (NEB), **Lane 5:** dsRNA (Ambion), **Lane 6:** Negative control (no enzyme), **Lane 7:** Negative control (no template).
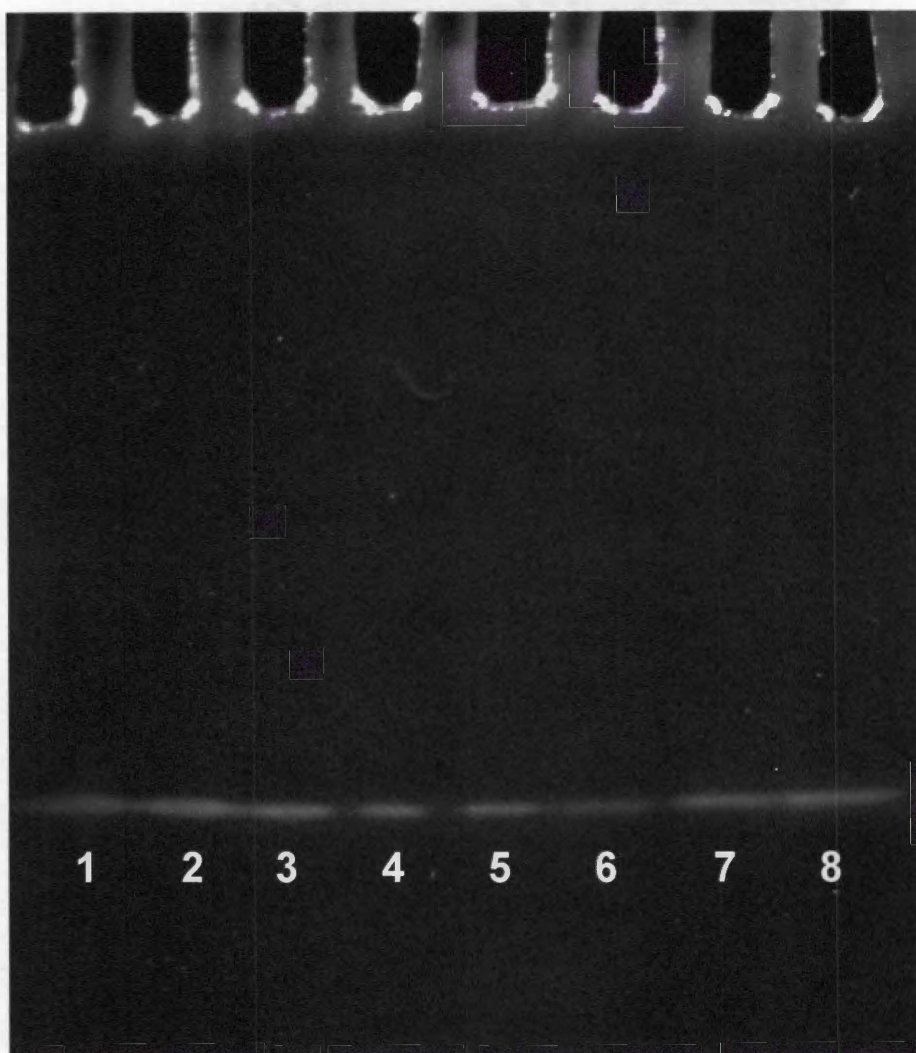
Figure 22. Quantification and integrity of siRNA. Serial dilution of double stranded DNA oligo, 20µM stock, used to quantify and measure the integrity of the siRNA generated from the NEB and Ambion RNAse III enzymes. 12% non-denaturing polyacrylamide gel stained with ethidium bromide. **Lane 1:** 10µl, 20µM DNA oligo, **Lane 2:** 10µl, 10µM DNA oligo, **Lane 3:** 10µl, 4µM DNA oligo, **Lane 4:** 10µl, 2µM DNA oligo, **Lane 5:** 10µl, 1µM DNA oligo, **Lane 6:** 10µl Bcr-Abl NEB RNAse III enzyme product, **Lane 7:** 10µl Bcr-Abl Ambion RNAse III enzyme product, **Lane 8:** 10µl Lit28mal Ambion RNAse III enzyme product.

Oligofectamine

RNAifect

A.

B.
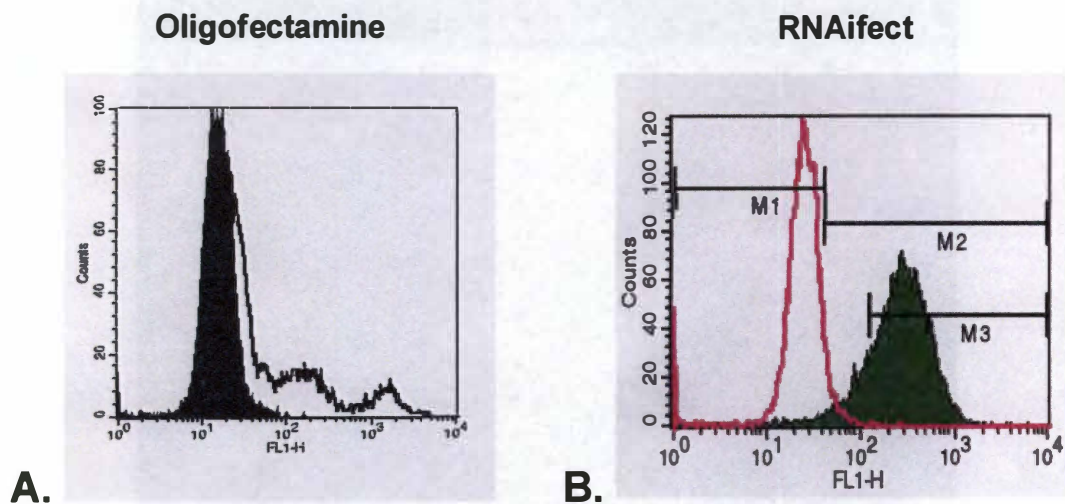
Figure 23: Transfection efficiency by flow cytometry. Transfection efficiency as measured using a non-silencing fluorescein conjugated siRNA duplex through flow cytometry. **Panel A:** Closed region represents the untransfected control, open area represents the Oligofectamine transfected K-562 cells. Oligofectamine yielded a 25% transfection efficiency. **Panel B:** Open area represents the untransfected control, the closed green area represents the K-562 cells transfected using RNAifect. RNAifect yielded a transfection efficiency of 90%. Both transfection reagents were repeated several times with similar results.

51
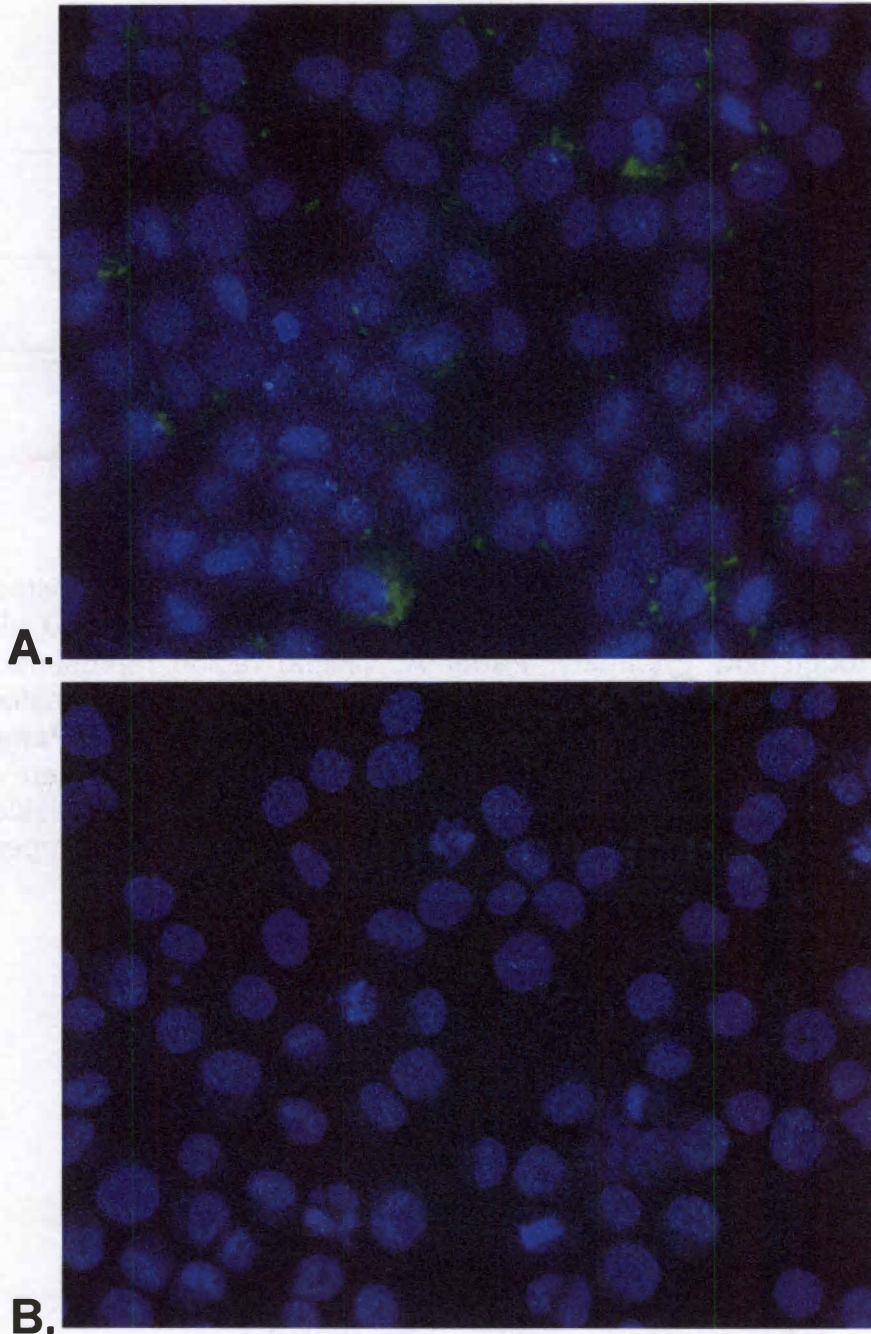
Figure 24. Transfection efficiency by fluorescent microscopy. Fluorescent microscopy, 400X total magnification, of K-562 cells transfected with a non-silencing fluorescein-conjugated siRNA stained with Hoescht 33324. **Panel A:** fluorescein-conjugated siRNA, **Panel B:** untransfected control

The RNAi effect was measured using three approaches, including serial dilution of the RNA, real time PCR, and western blotting to measure the modulation of the Bcr-Abl protein. The lowest detectable *Bcr-Abl* transcript concentration of K-562 RNA was determined through a serial dilution of the RNA in the RT-PCR reaction. Concentrations of RNA were high enough to show the presence of the Bcr-Abl transcript product, and low enough to illustrate the difference between the RNAi treated cells and the untreated. The results of this dilution show that the lowest concentration to visualize the *Bcr-Abl* transcript product on an agarose gel is at 3μg/ml RNA in the RT-PCR reaction (Figure 25). This dilution series was then applied to K-562 RNA transfected with both synthetic and transcribed Bcr-Abl-specific siRNA at 48 hours (Figure 26). The RNAi effect is visible with 5μg/ml RNA in the RT-PCR, where both the transcribed and the synthetic *Bcr-Abl*-specific siRNA treated cells have less *Bcr-Abl* transcript than the untreated control. When compared to the irrelevant and the untreated control in Figure 27, both the synthetic and the transcribed Bcr-Abl-specific siRNA treated cells showed a remarkable drop in the amount of Bcr-Abl transcript, and no relative change in the *Aldolase* transcript.

The visible reduction in *Bcr-Abl* transcript levels was confirmed to be due to mRNA degradation using real time PCR to quantify the levels of *Bcr-Abl* transcript and the housekeeping gene *GAPDH* as a control. The synthetic *Bcr-Abl*-siRNA mRNA was silenced 70% and the transcribed-digested *Bcr-Abl*-siRNA resulted in a 50% knockdown of the *Bcr-Abl* mRNA (Figure 28).
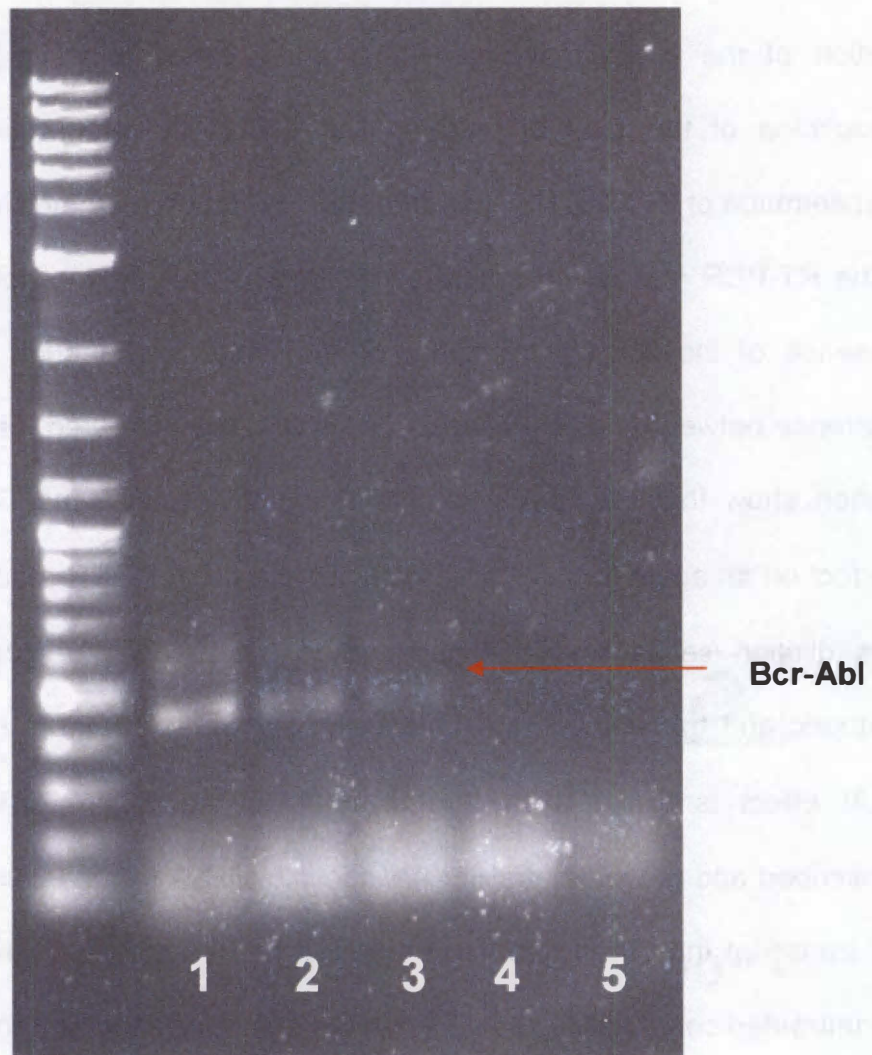
Bcr-Abl

Figure 25: Bcr-Abl RNA threshold. Serial dilutions of total RNA in RT-PCR reactions established the range of detection of the *Bcr-Abl* gene down to 60ng (3μg/ml) template RNA. 1.5% agarose gel stained with ethidium bromide **Lane 1:** 12.5 μg/ml RNA, **Lane 2:** 6.25 μg/ml RNA, **Lane 3:** 3 μg/ml RNA, **Lane 4:** 1.5 ng RNA, **Lane 5:** negative reaction control (no template)

Titration of RNA (µg/ml) in RT-PCR to show RNAi Effect at 48 hours

5µg 10µg 20µg 40µg

A.

B.

C.

D.
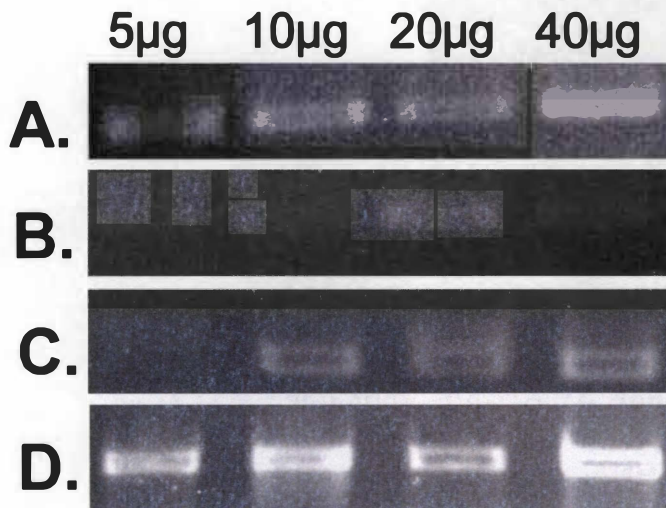
Figure 26. RNAi through RT-PCR at 48 hours. PCR of titration of RNA in RT-PCR illustrates the degradation of the *Bcr-Abl* mRNA at the 5µg/ml concentration, 1.5% agarose gel stained with ethidium bromide. **Panel A:** untreated, *Bcr-Abl* fragment, **Panel B:** synthetic *Bcr-Abl*-specific siRNA (800nM), *Bcr-Abl* fragment, **Panel C:** transcribed *Bcr-Abl*-specific siRNA (800nM), *Bcr-Abl* fragment, **Panel D:** untreated, *Aldolase* fragment

RNAi Effect at 72 hours
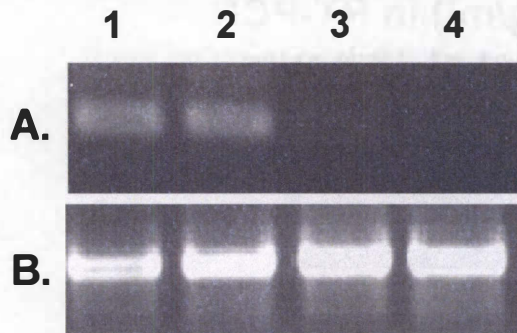
Figure 27. RNAi at 72 hours. PCR of RT-PCR using 5µg/ml total RNA harvested from K-562 cells at 72 hours shows the degradation of Bcr-Abl mRNA, 1.5% agarose gel stained with ethidium bromide. **Panel A:** *Bcr-Abl* fragment, **Panel B:** *Aldolase* fragment. **Lane 1:** untreated, **Lane 2:** irrelevant siRNA (800nM), **Lane 3:** synthetic *Bcr-Abl*-specific siRNA (800nM), **Lane 4:** transcribed *Bcr-Abl*-specific siRNA (800nM)

Bcr-Abl mRNA at 48 hours
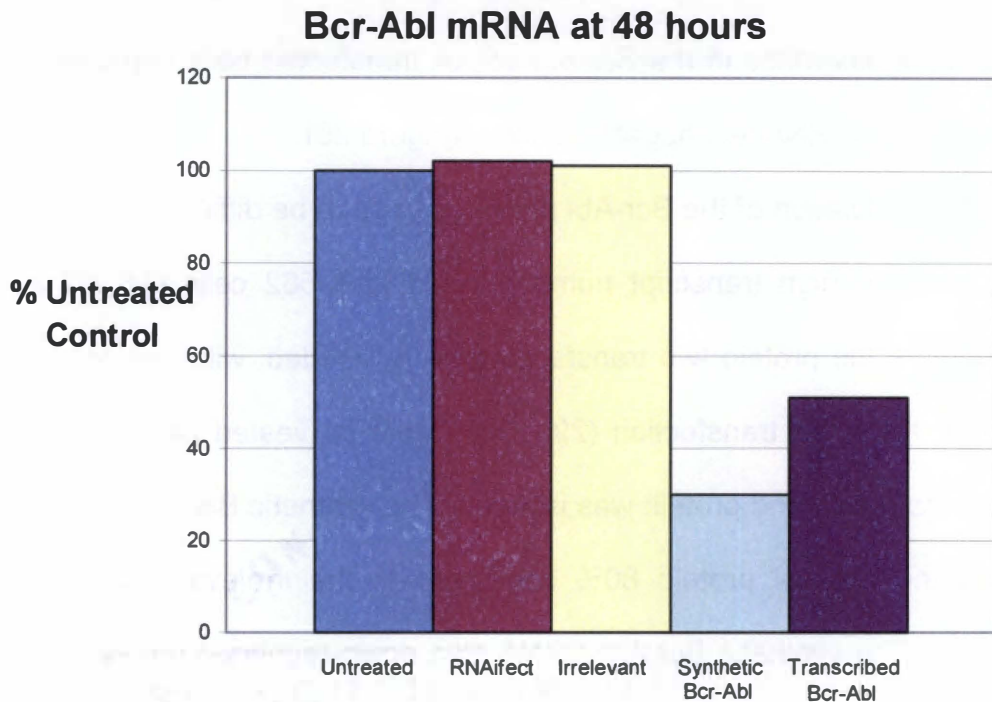
Figure 28. Real time PCR measuring *Bcr-Abl*. Real time PCR data for *Bcr-Abl* mRNA of K-562 cells transfected with 4μg siRNA illustrates that the synthetic Bcr-Abl-specific siRNA reduced the *Bcr-Abl* mRNA of K-562 cells 70% and the transcribed *Bcr-Abl* siRNA reduced the *Bcr-Abl* mRNA 50%, while the negative controls show no change of *Bcr-Abl* mRNA levels in relation to the untreated control.

Using the *GAPDH* as the housekeeping gene control, there was an unremarkable difference in the *Bcr-Abl* siRNA transfected cells compared to the untreated and the RNAifect negative control (Figure 29).

The modulation of the Bcr-Abl protein proved to be difficult due to the long half-life and the high transcript number found in K-562 cells (15, 27-29). To down-regulate the protein two transfections were needed, with one following 24 hours after the initial transfection (29). Cells were harvested 24 hours after the second transfection and protein was isolated. The synthetic Bcr-Abl siRNA down-regulated the Bcr-Abl protein 80% compared to the irrelevant siRNA control (Figure 30). The synthetic Bcr-Abl siRNA also down-regulated the Bcl-$_{XL}$ protein greater than 75% compared to the irrelevant siRNA control, suggesting an induction of apoptosis (Figure 30).

Combination Treatment

Alone, RNAi and Gleevec are effective, respectively, at reducing the amount of Bcr-Abl mRNA and protein. When combined they show possible synergism. Proliferation and apoptosis measurements were used to show the synergistic relationship between RNAi and Gleevec. The initial findings supported Bcr-Abl-specific siRNA and Gleevec interacting, but the effect was minimal at 800nM siRNA (Figure 31). When the higher concentration of 1.6 μM siRNA was combined with Gleevec, the RNAi specifically lowered the IC$_{50}$ greater than 2-fold at both 48 and 72 hours compared to the negative control (Figures 32 and 33). Based on the proliferation dose response curve established for Gleevec

GAPDH mRNA at 48 hours
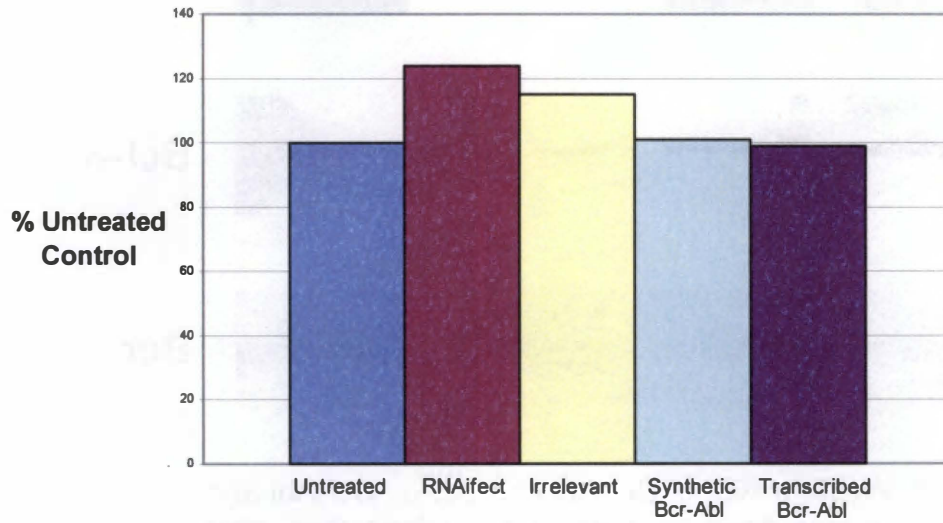
Figure 29. Real time PCR measuring *GAPDH*. Real time PCR data for *GAPDH* mRNA of K-562 cells transfected with 4µg siRNA illustrates that there is little effect on transcription of the housekeeping gene, *GAPDH* as a result of transfection with these siRNA.
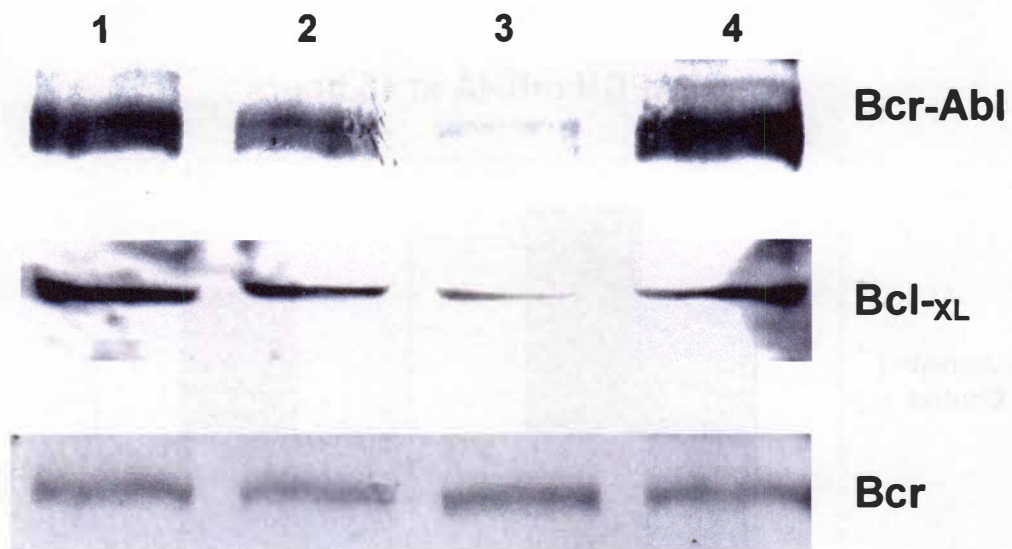
Figure 30. Western Blot of Bcr-Abl and Bcl-$_{XL}$. Bcr-Abl and Bcl-$_{XL}$ protein was down-regulated greater than 80% after two transfections of synthetic *Bcr-Abl*-specific siRNA. Bcr was used as a loading control. **Lane 1:** RNAifect alone, **Lane 2:** Irrelevant siRNA (4µg), **Lane 3:** synthetic *Bcr-Abl*-specific siRNA (4µg), **Lane 4:** transcribed-digested Bcr-Abl-specific siRNA (4µg)

Combination Treatment at 72 Hours
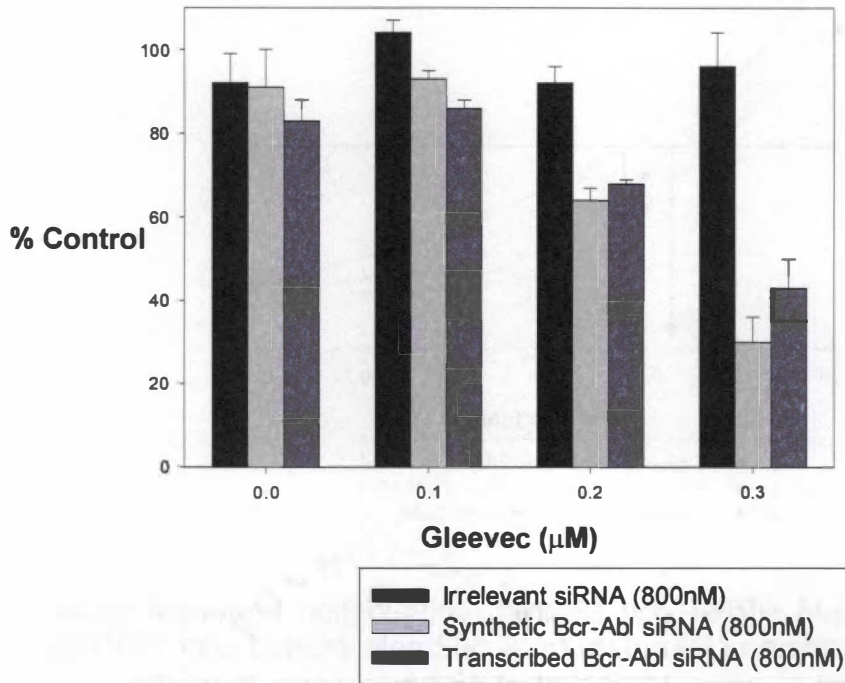
Figure 31. 800nM siRNA combination treatment at 48 hours. [³H]-thymidine uptake data for K-562 cells treated with 800nM siRNA as normalized to the negative control (RNAifect alone) at 72 hours illustrates that as the doses of Gleevec increase, the synthetic and transcribed-digested Bcr-Abl siRNA show a decline in proliferation.
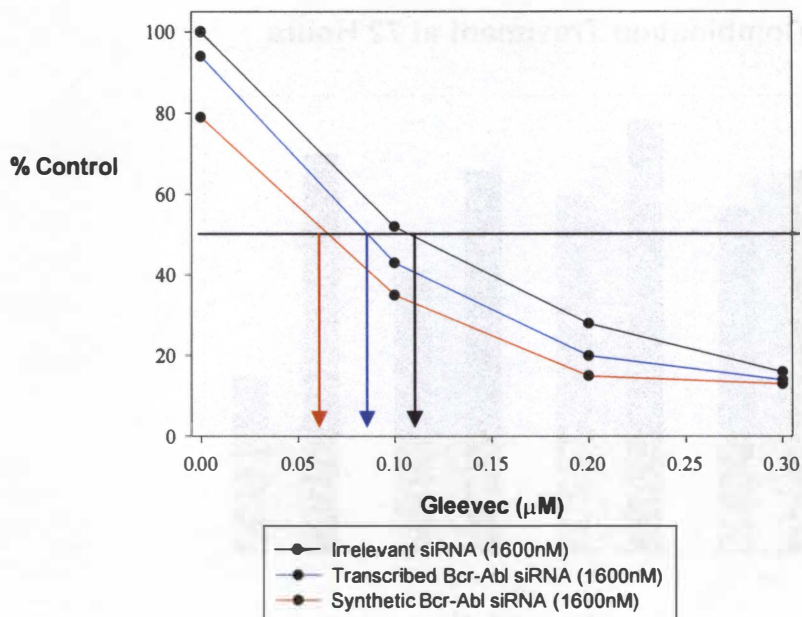
Figure 32. 1.6μM siRNA and Gleevec combination treatment at 48 hours. [³H]-thymidine uptake data for K-562 cells treated with 1600nM siRNA compared to negative control at 48 hours show a greater than two-fold decline in proliferation of the cells transfected with Bcr-Abl-specific siRNA compared to those transfected with irrelevant siRNA.

Combination Treatment at 72 hours
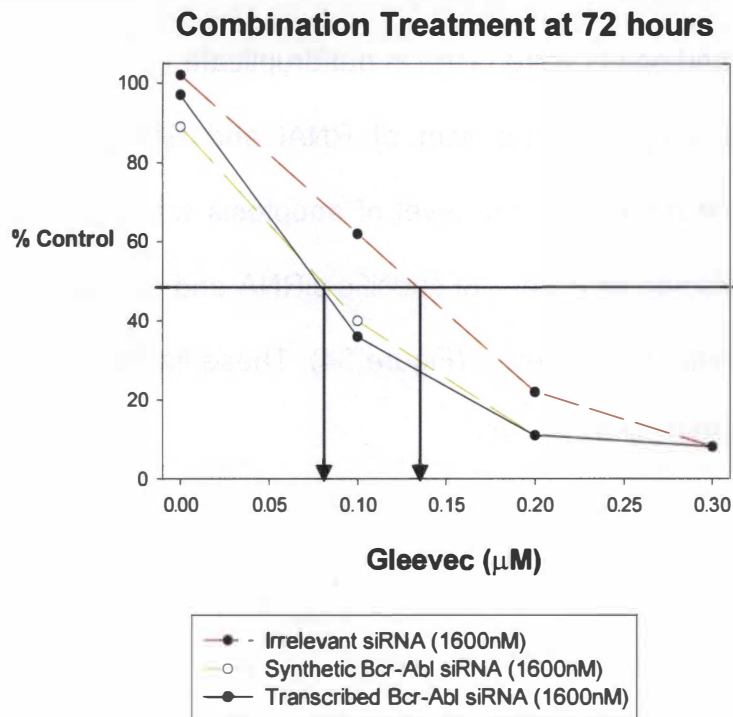
Figure 33. 1.6μM siRNA and Gleevec combination treatment at 72 hours. [^{3}H]-thymidine uptake data for K-562 cells treated with 1600nM siRNA compared to negative control at 72 hours show a greater than two-fold decline in proliferation of the cells transfected with Bcr-Abl-specific siRNA compared to those transfected with irrelevant siRNA.

(Figures 7, 8, 9, and 10) the IC_{50} was lowered greater than 3-fold. Experiments were repeated three times and points were taken in quadruplicate.

The apoptosis data supports synergism of RNAi and Gleevec. When functional mitochondria were measured, the level of apoptosis was significantly greater in K-562 cells transfected with Bcr-Abl specific siRNA and apoptosis was observed at lower concentrations of Gleevec (Figure 34). These findings suggest a correlation with Bcr-Abl siRNA and Gleevec.

Combination Treatment Effect on Apoptosis at 72 hours
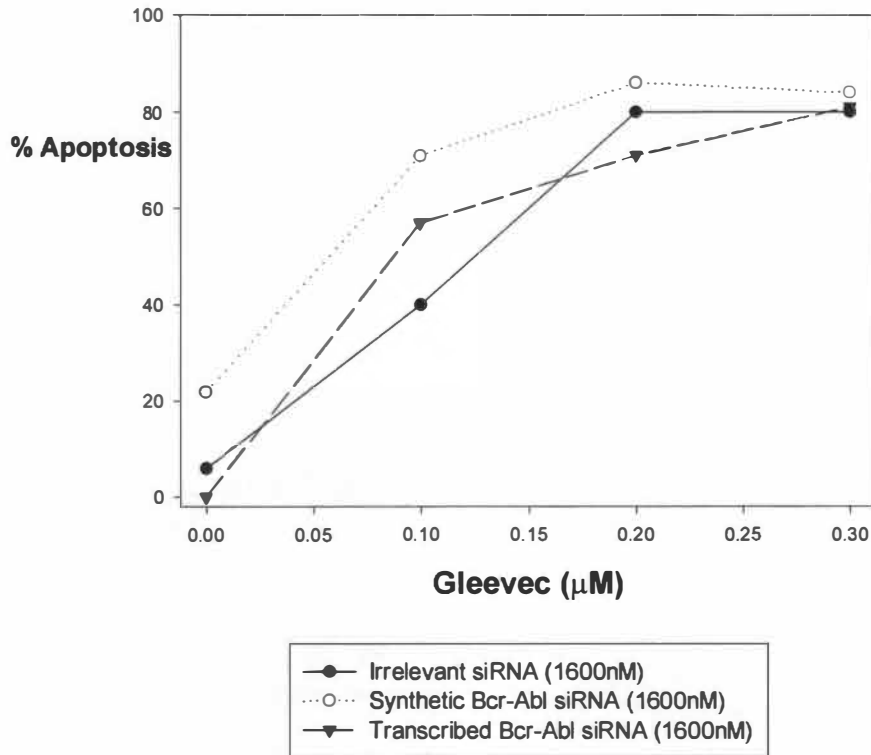
Figure 34. 1.6µM siRNA and Gleevec treatment induces apoptosis. Apoptosis was determined by functional mitochondria assay of K-562 cells co-treated with 1600nM siRNA and Gleevec presented as percent of the untreated control at 72 hours.

Chapter 4

Discussion

RNAi has been established as a means to silence the transcription and subsequent translation of a gene both *in vitro* and *in vivo* (2, 4, 18, 19, 28, 29). The *Bcr-Abl* translocation is a potent transforming agent in leukemogenesis and many studies have focused on its down-regulation (34, 40, 57, 144). Studies involving antisense and RNAi have been effective in down-regulating the *Bcr-Abl* oncogene *in vitro* (15, 28, 29, 118). The tyrosine kinase inhibitor, Gleevec, has proven to be an effective inhibitor of the Bcr-Abl protein (32). In this study, both Gleevec and RNAi targeted the Bcr-Abl protein and gene, respectively, allowing for both upstream and direct modulation of the same molecular target.

Previous studies aimed at Bcr-Abl mRNA knockdown have been effective at abrogating the translation of the Bcr-Abl protein (14, 15, 118). The down-regulation of the Bcr-Abl mRNA restored sensitivity to apoptosis (118, 141). Antisense approaches have been effective at down-regulating the *Bcr-Abl* oncogene in CML primary cells and K-562 cells and have been approved for clinical trials (15, 118, 142). Spiller *et al.* reported significant mRNA transcript reduction using modified antisense ODN specific for the *Bcr-Abl* fusion site, although no change in Bcr-Abl expression was observed (15). Protein down-regulation was unchanged, probably due to the transient nature and instability of the ODN as well as the long half-life of the Bcr-Abl protein, which has been

reported at being greater than 48 hours (15, 117). Martiat *et al.* demonstrated that the stable expression of the antisense ODN specific for the *Bcr-Abl* fusion site delivered using a retroviral vector in K-562 cells resulted in a decline in proliferation coupled with down-regulation of *Bcr-Abl* mRNA and protein (118). A constant antisense presence resulted in the Bcr-Abl protein down-regulation.

RNAi offers an alternative approach to repress the translation of a specific gene, which involves the specific degradation of targeted mRNA (10, 19). While RNAi approaches differ from antisense in the mechanism of action, both result in translational inhibition. RNAi has proven successful in knocking down the *Bcr-Abl* oncogene, abrogating the production of the Bcr-Abl protein (28, 29, 113). In this study, RNAi was selected to inhibit the Bcr-Abl gene due to the stability of double stranded siRNA *in vitro*. Two different siRNA preparations were compared to measure the Bcr-Abl gene knockdown.

The efficacy of siRNA delivery into the targeted cell was critical, and there have been several developments aimed at increasing the efficiency of delivery (113, 143). Initial experiments with Oligofectamine and Lipofectamine 2000 were 25% and 5% effective, respectively, as measured by the uptake of a non-silencing fluorescein-conjugated siRNA duplex by flow cytometry (Figure 22). These experiments were performed in serum-free media, which could have contributed to low transfection efficiency. Transfection with RNAifect yielded over 90% siRNA oligonucleotide uptake in the presence of serum and was selected because the transfection conditions were most similar to culture conditions (Figure 22).

68

Two *Bcr-Abl*-specific siRNA preparations spanning the Bcr-Abl fusion site were compared to evaluate the efficacy of both the synthetic (Qiagen) and transcribed-digested, which we prepared (28, 29, 140). The transcribed-digested siRNA were generated from a 450 bp fragment spanning the *Bcr-Abl* fusion site, which yielded a heterogeneous mixture of siRNA, 17-19 nucleotides in length. The transcribed-digested preparation encompassed more than the homogenous Bcr-Abl breakpoint-specific synthetic siRNA with the anticipation that it would offer other sites of gene down-regulation with a single transfection. *Bcr-Abl* mRNA levels were measured both qualitatively through RT-PCR and quantitatively through real time PCR. The transcribed-digested *Bcr-Abl* siRNA resulted in a 50% down-regulation of the *Bcr-Abl* mRNA measured by real time PCR (Figure 27) and *Bcr-Abl* was not detected using RT-PCR. This supported Yang *et al.*, who observed significant luciferase gene knockdown using transcribed-digested siRNA (140). The heterogeneity of our transcribed-digested Bcr-Abl siRNA proved to be a disadvantage and was not observed to down-regulate the Bcr-Abl protein. The heterogeneity of the transcribed-digested siRNA could have diluted the effective domains for potent silencing and, as a result, there were less siRNA specific for regions that would have produced a greater effect.

Synthetic Bcr-Abl siRNA-transfected cells showed a 70% reduction of Bcr-Abl mRNA, as measured through real time PCR and were undetected using RT-PCR, suggesting a more potent knockdown of the Bcr-Abl mRNA (Figure 27). These results corroborate Wilda *et al.* and Scherr *et al.*, who both reported 70%

Bcr-Abl mRNA knockdown using synthetic siRNA, and Li *et al.*, who reported greater than 90% Bcr-Abl knockdown with shRNA (28, 29, 113). The synthetic Bcr-Abl siRNA were also capable of down-regulating both the Bcr-Abl and Bcl-$_{XL}$ proteins (Figure 29). Oetzel *et al.* observed that down-regulation of the Bcr-Abl protein by Gleevec led to down-regulation of Bcl-$_{XL}$ protein (34). This suggested that sensitivity to apoptosis had been reversed, as well as underscored the well-defined relationship of Bcr-Abl and Bcl-$_{XL}$ in K-562 cells (34, 39, 57, 114). As was observed by Scherr *et al.*, the synthetic Bcr-Abl siRNA required a second transfection 24 hours later to down-regulate the Bcr-Abl protein (29). The dilution of the siRNA through cell divisions and the long half-life of the Bcr-Abl protein necessitated a second transfection to deliver the siRNA into the newly divided cells.

Initial studies were focused on determining the proliferative and apoptotic effects of varying concentrations of Gleevec in K-562 cells. The antiproliferative effect of Gleevec was attributed to specific inhibition of the Bcr-Abl tyrosine kinase (32-37). The range where the effect of Gleevec would not mask the effect of RNAi when combined was determined through a dose-response curve of Gleevec daily, over 4 days. These initial studies, measured by proliferation assays in K-562 cells co-cultured with Gleevec, determined the IC$_{50}$ to be 0.2 μM and demonstrated that 48 hours and 72 hours were the optimal times to observe the antiproliferative effect (Figures 7 and 8). This dose corroborated Buchdunger *et al.* who reported 0.25 μM as the IC$_{50}$ of Gleevec (35). Time-points were also taken at both 24 and 96 hours, where results at 24 hours were unremarkable and

70

96 reflected an increase in apoptosis. Apoptosis was measured daily over 4 days in cells co-cultured with Gleevec. Both caspase 3 activity and mitochondrial membrane collapse were elevated as the concentration of Gleevec increased. The apoptosis data corroborated 48 and 72 hours as the optimal times to observe the apoptotic effects of Gleevec in K-562 cells (Figures 9-12). The correlation with decline in proliferation and increase in apoptosis suggested that Gleevec induced apoptosis in K-562 cells (Figures 13 and 14). There was no marked effect in either parameter at 24 hours, and at 96 hours even the control was showing an increase in apoptosis.

Studies investigating the combination of Bcr-Abl-specific siRNA with Gleevec involved 3 doses that spanned the IC_{50}. Proliferation was used to measure the correlation of siRNA-transfected cells treated with Gleevec because the initial studies establishing the IC_{50} measured proliferation. The findings suggested a correlation between the combination of both synthetic and transcribed-digested Bcr-Abl-specific siRNA and Gleevec in K-562 cells. The established Gleevec IC_{50} was lowered from $0.2\mu M$ to $0.06\mu M$ when treated with $4\mu g$ $(1.6\mu M)$ *Bcr-Abl*-specific siRNA, and unaffected with $4\mu g$ $(1.6\mu M)$ irrelevant Lit28mal siRNA, suggesting an association between Gleevec and *Bcr-Abl* siRNA (Figures 32 and 33). Lower concentrations of siRNA at $2\mu g$ (800nM) resulted in a lesser effect, which suggests that the siRNA act in a concentration-related manner (Figure 31). The proposed mechanism for this interaction involves the degradation of the *Bcr-Abl* mRNA, leading to a decrease in the production of the Bcr-Abl protein as shown in Figure 35. The amount of Gleevec required to inhibit

the remaining Bcr-Abl protein was reduced because production of the protein had been inhibited. An increase of apoptosis in cells transfected with both *Bcr-Abl-*specific siRNA and treated with Gleevec was greater than the level of apoptosis observed in cells treated with Gleevec alone (Figure 34). Higher amounts of siRNA used in the transfections were determined to be cytotoxic at levels greater than 4μg (data not included), probably due to the higher levels of RNAifect required for complex formation. These results were similar to those observed by Scherr *et al.*, who found that synthetic Bcr-Abl siRNA delivered using electroporation sensitized *Bcr-Abl-*positive BaF3 cells for treatment with Gleevec (30).

In conclusion, this study suggested a correlation with transfection of K-562 cells with Bcr-Abl-specific siRNA and treatment with Gleevec. The results showed that the effective dose of Gleevec was lowered greater than two-fold when primed with Bcr-Abl-specific siRNA. While both siRNA preparations exhibit this correlation, the synthetic siRNA preparation resulted in a greater reduction of the mRNA. The synthetic Bcr-Abl siRNA required two transfections to down-regulate the Bcr-Abl protein, while the transcribed-digested showed no effect on the Bcr-Abl protein. To corroborate the down-regulation of Bcr-Abl, Bcl-$_{XL}$ protein levels were also reduced in K-562 cells transfected twice with synthetic Bcr-Abl siRNA, suggesting that apoptosis sensitivity was restored.
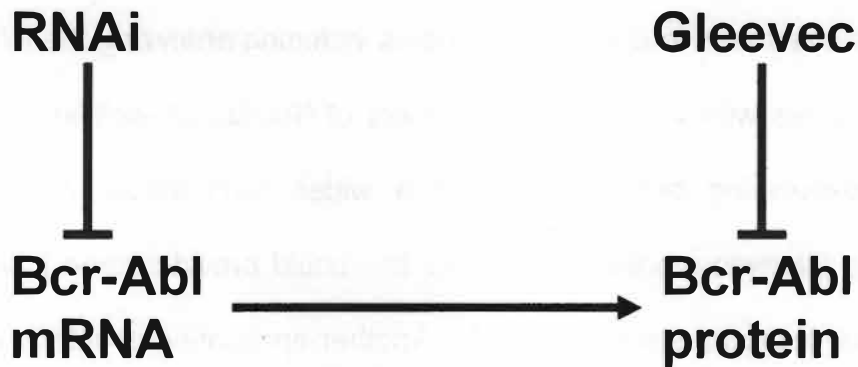
Figure 35. Proposed RNAi/Gleevec mechanism. The proposed mechanism of RNAi lowering the IC_{50} of Gleevec involves the degradation of the Bcr-Abl transcript by Bcr-Abl specific siRNA. The reduction of the Bcr-Abl transcript leads to a reduction in the Bcr-Abl protein. With less of the Bcr-Abl protein present, a lower dose of Gleevec is required to inhibit proliferation.

Proposed Further Studies

This project could lead to a variety of studies including analyzing the RNAi effect in K-562 sublines with varying copy numbers of Bcr-Abl as well as using different Bcr-Abl-expressing cell lines to get a wider comparison. A study applying RNAi in a Gleevec-resistant K-562 cell line could provide some insight on the mechanisms of drug resistance in CML. Another application could involve using Bcr-Abl mutants and measuring the efficacy of RNAi specific for Bcr-Abl. Studies involving a dual RNAi approach using siRNA for both Bcl-$_{XL}$ and for Bcr-Abl could be analyzed to determine if there is an additive relationship between the two siRNAs.

References

1.   Couzin J. Small RNAs Make Big Splash. *Science* 298: 2296, 2002.

2.   Fire A, Xu S, Montgomery M. Potent and Specific Genetic Interference by Double-Stranded RNA in Caenorhabditis elegans. *Nature* 391: 806, 1998.

3.   Ramaswamy G, Slack F. siRNA: A Guide for RNA Silencing. *Chemistry and Biol.* 9: 1053, 2002.

4.   Elbashir S, Harborth J, Lendeckel W et al. Duplexes of 21-nucleotide RNAs Mediate RNA Interference in Cultured Mammalian Cells. *Nature* 411: 494, 2001.

5.   Elbashir S, Lendeckel W, Tuschl T. RNA Interference is Mediated by 21- and 22-nucleotide RNAs. *Genes and Development* 15: 188, 2001.

6.   Lipardi C, Wei Q, Paterson B. RNAi as Random Degrative PCR: siRNA Primers Convert mRNA into dsRNAs that are Degraded to Generate New siRNAs. *Cell* 107: 297, 2001.

7.   Ding SW. RNA Silencing. *Current Opinion in Biotechnology* 11: 152, 2000.

8.   Timmons L. The Long and Short of siRNAs. *Molecular Cell* 10: 435, 2002.

9.   Lin S-L, Chuong C-M, Ying S-Y. A Novel mRNA-cDNA Interference Phenomneon for Silencing bcl-2 Expression in Human LNCaP Cells. *Biochemical and Biophysical Research Communications* 281: 639, 2001.

10.   Waterhouse P, Helliwell C. Exploring Plant Genomes by RNA-induced Gene Silencing. *Nature Genetics* 4: 29, 2003.

11.   Conklin D. RNA-Interference-Based Silencing of Mammalian Gene Expression. *Chembiochem* 4: 1033, 2003.

12.   Gitlin L, Karelsky S, Andino R. Short Interfering RNA Confers Intracellular Antiviral Immunity in Human Cells. *Nature* 418: 430, 2002.

13.   Hill J, Ichim T, Kusznieruk K et al. Immune Modulation by Silencing IL-12 Production in Dendritic Cells Using Small Interfering RNA. *Journal of Immunology* 171: 691, 2003.

14.   Weiss B, Davidkova G, Zhou L-W. Antisense RNA Gene Therapy for Studying and Modulating Biological Processes. *Cell. Mol. Life Sci.* 55: 334, 1999.

15.   Spiller D, Giles R, Grzybowski J et al. Improving the Intracellular Delivery and Molecular Efficacy of Antisense Oligonucleotides in Chronic Myelogenous Leukemia Cells: a Comparison of Streptolysin-O Permeabilization, Electroporation, and Lipophilic Conjugation. *Blood* 91 (12): 4738, 1998.

16.   Far R, Sczakiel G. The Activity of siRNA in Mammalian Cells is Related to Structural Target Accessibility: a Comparison with Antisense Oligonucleotides. *Nucleic Acids Research* 31 (15): 4417, 2003.

17.   Zhang Y, Boado R, Pardridge W. In vivo Knockdown of Gene Expression in Brain Cancer with Intravenous RNAi in Adult Rats. *J Gene Med* 5: 1039, 2003.

18.   Sorensen D, Leirdal M, Sioud M. Gene Silencing by Systemic Delivery of siRNAs in Adult Mice. *J. Mol. Biol.* 327: 761, 2003.

19.   McManus M, Sharp P. Gene Silencing in Mammals by Small Interfering RNAs. *Nature Genetics* 3: 737, 2002.

20. Szweykowska-Kulinska Z, Jarmolowski A, Figlerowicz. RNA Interference and its Role in the Regulation of Eucaryotic Gene Expression. *Acta Biochemica Polonica* 50 (1): 217, 2003.

21. Sawyers C. Chronic Myelogenous Leukemia. *New England Journal of Medicine* 340 (17): 1330, 1999.

22. Nowell P. A Minute Chromosome in Human Chronic Granulocytic Leukemia. *Science* 132 (3438): 1488, 1960.

23. Rowley JD. Letter: A New Consistent Chromosomal Abnormality in Chronic Myelogenous Leukaemia Identified by Quinacrine Fluorescence and Giemsa Staining. *Nature* 243 (5405): 290, 1973.

24. Laurent E, Moshe T, Hagop K et al. The BCR Gene and Philadelphia Chromosome-positive Leukemogenesis. *Cancer Research* 61: 2343, 2001.

25. Cioca D, Aoki Y, Kiyosawa K. RNA Interference is a Function Pathway with Therapeutic Potential in Human Myeloid Leukemia Cell Lines. *Cancer Gene Therapy* 10: 125, 2003.

26. Damm-Welk, Fuchs U, Wossman W et al. Targeting Oncogenic Fusion Genes in Leukemias and Lymphomas by RNA Interference. *Seminars in Cancer Biology* 13: 283, 2003.

27. Moracova J, Nadvornikova-Muchova S, Brezinova J. Overproduction of BCR-ABL Transcripts in Human Leukemic Cell Lines K-562 and BV173. *Eur. J. Haematol.* 64: 135, 2000.

28. Wilda M, Fuchs U, Wossman et al. Killing of Leukemic Cells with a BCR/ABL Fusion Gene by RNA Interference (RNAi). *Oncogene* 21: 5716, 2002.

29. Scherr M, Battmer K, Heidenreich O et al. Specific Inhibition of Bcr-Abl Gene Expression by Small Interfering RNA. *Blood* 101 (4): 1566, 2003.

30. Wohlbold L, van der Kuip H, Miething C et al. Inhibition of bcr-abl Gene Expression by Small Interfering RNA Sensitizes for Imatinib Mesylate (STI571). *Blood* 102 (6): 2236, 2003.

31. Tseng C-P, Huang C-L, Huang C-H et al. Disabled-2 Small Interfering RNA Modulates Cellular Adhesive Function and MAPK Activity during Megakaryocytic Differentiation of K-562 Cells. *FEBS Letters* 541: 21, 2003.

32. Manley PW, Cowan-Jacob SW, Buchdunger E et al. Imatinib: a Selective Tyrosine Kinase Inhibitor. *Eur. J Cancer* 38 (supp 5): S19, 2002.

33. Druker B. Imatinib and Chronic Myeloid Leukemia: Validating the Promise of Molecularly Targeted Therapy. *Eur. J Cancer 38 (supp 5):* S70, 2002.

34. Oetzel C, Jonuleit T, Gotz A et al. *The Tyrosine* Kinase Inhibitor CGP 57148 (STI 571) Induces Apoptosis in BCR-ABL-positive Cells by Down-Regulating BCL-X. *Clinical Cancer Research* 6: 1958, 2000.

35. Buchdunger E, O'Reilly T, Wood J. Pharmacology of Imatinib (STI571). *Eur J Cancer* 38 (supp 5): S28, 2002.

36. Peggs K, Mackinnon S. Imatinib Mesylate – The New Gold Standard for Treatment of Chronic Myeloid Leukemia. *N Engl J Med* 348 (11): 1048, 2003.

37. Fang G, Kim C, Perkins C et al. CGP57148B (STI-571) Induces Differentiation and Apoptosis and Sensitizes Bcr-Abl-positive Human Leukemia Cells to Apoptosis due to Antileukemic Drugs. *Blood* 96 (6): 2246, 2000.

38. McGahon A, Nishioka W, Martin S et al. Regulation of the Fas Apoptotic Cell Death Pathway by Abl. *Journal of Biological Chemistry* 270 (38): 22625, 1995.

39. Amarante-Mendés G, McGahon A, Nishioka W et al. Bcl-2-independent Bcr-Abl-mediated Resistance to Apoptosis: Protection is Correlated with Up Regulation of Bcl-X_L. *Oncogene* 16 (11): 1383, 1998.

40. Topaly J, Zeller WJ, Fruehauf S. Combination Therapy with Imatinib Mesylate (STI571): Synopsis of In Vitro Studies. *British Journal of Haematology* 119: 3, 2002.

41. Sun X, Layton J, Elefanty A et al. Comparison of Effects of the Tyrosine Kinase Inhibitors AG957, AG490, and STI571 on BCR-ABL-expressing Cells, Demonstrating Synergy Between AG490 and STI571. *Blood* 97 (7): 2008, 2001.

42. Mathias C, Wakoff A, Porter D. Chronic Myelogenous Leukemia: Extending the *Prospects for Cure. Hosp. Pract.* June 15: 137, 1998.

43. Wertheim J, Miller J, Xu L et al. The Biology of Chronic Myelogenous Leukemia: Mouse Models and Cell Adhesion. *Oncogene* 21: 8612, 2002.

44. Johansson B, Fioretos T, Mitelman F. Cytogenetic and Molecular Genetic Evolution of Chronic Myelogenous Leukemia. *Acta Haematol.* 107: 76, 2002.

45. Iolascon A, Ragione F, Giordani L et al. Expression of Cell Cycle Regulatory Genes in Chronic Myelogenous Leukemia. *Haematologica* 83: 771, 1998.

46. Melo J. The Diversity of BCR-ABL Fusion Proteins and Their Relationship to Leukemia Phenotype. *Blood* 88 (7): 2375, 1996.

47. Salesse S, Verfaille C. Bcr/Abl: from Molecular Mechanisms of Leukemia Induction to Treatment of Chronic Myelogenous Leukemia. *Oncogene* 21: 8547, 2002.

48. Zamecnikova A. Chronic Myelogenous Leukemia as Gene Activation Model in Oncology Minireview. *Neoplasma* 47 (5): 269, 2000.

49. Campbell M, Li W, Arlinghaus R. P210 BCR-ABL is Complexed to P160 BCR and ph-P53 Proteins in K-562 Cells. *Oncogene* 5: 773, 1990.

50. Druker B, Lydon N. Lessons Learned from the Development of an Abl Tyrosine Kinase Inhibitor for Chronic Myelogenous Leukemia. *Journal of Clinical Investigation* 105: 3, 2000.

51. Steelman LS, Pohnert SC, Shelton JG et al. JAK/STAT, Raf/MEK/ERK, PI3K/Akt and Bcr-Abl in Cell Cycle Progression and Leukemogenesis. *Leukemia* 18: 189, 2004.

52.   Jorgensen H, Holyoake T. A Comparison of Normal and Leukemic Stem Cell Biology in Chronic Myeloid Leukemia. *Hematological Oncol.* 19: 89, 2001.

53.   Xie S, Wang Y, Liu J et al. Involvement of Jak2 Tyrosine Phosphorylation in Bcr-Abl Transformation. *Oncogene* 20: 6188, 2001.

54.   Kabarowski J, Witte O. Consequences of Bcr-Abl Expression within the Hematopoietic Stem Cell in Chronic Myelogenous Leukemia. *Stem Cells* 18: 399, 2000.

55.   Dickens M, Rogers J, Cavanagh J et al. A Cytoplasmic Inhibitor of the JNK Signal Transduction Pathway. *Science* 277: 693, 1997.

56.   Perroti D, Calabretta B. Post-Transcriptional Mechanisms in Bcr/Abl Leukemogenesis: Role of Shuttling RNA-binding Proteins. *Oncogene* 21: 8577, 2002.

57.   Sattler M, Griffin J. Molecular Mechanisms of Transformation by the Bcr-Abl Oncogene. *Semin Hematol* 40 (suppl 2): 4, 2003.

58.   Arlinghaus R. Bcr: A Negative Regulator of the Bcr-Abl Oncoprotein in Leukemia. *Oncogene* 21: 8560, 2002.

59.   Dorey K, Engen J, Kretzschmar J et al. Phosphorylation and Structure-Based Functional Studies Reveal a Positive and a Negative Role for the Activation Loop of the c-Abl Tyrosine Kinase. *Oncogene* 20: 8075, 2001.

60.   Nagar B, Hantschel O, Young M et al. Structural Basis for the Autoinhibition of c-Abl Tyrosine Kinase. *Cell* 112: 859, 2003.

61.   Lozzio C, Lozzio B. Human Chronic Myelogenous Leukemia Cell-Line With Positive Philadelphia Chromosome. *Blood* 45: 321, 1975.

62.   Klein E, Ben-Bassat H, Neumann H et al. Properties of the K562 Cell Line, Derived from a Patient with Chronic Myeloid Leukemia. *Int. J. Cancer* 18: 421, 1976.

63.   Wu S-Q, Voelkerding KV, Sabatini L et al. Extensive Amplification of Bcr/Abl Fusion Genes Clustered on Three Marker Chromosomes in Human Leukemic Cell Line K-562. *Leukemia* 9: 858, 1995.

64.   Hubbard S. Protein Tyrosine Kinases: Autoregulation and Small-molecule Inhibition. *Current Opinion in Structural Biology* 12: 735, 2002.

65.   Druker B. Imatinib As a Paradigm of Targeted Therapies. *Journal of Clinical Oncology* 21 (23s): 239, 2003.

66.   Ottman O, Hoezler D. The Abl Tyrosine Kinase Inhibitor STI571 (Glivec) in Philadelphia Positive Acute Lymphoblastic Leukemia – Promises, Pitfalls and Possibilities. *Hematology Journal* 3: 2, 2002.

67.   Schindler T, Bornmann W, Pellicena P et al. Structural Mechanism for STI-571 Inhibition of Ableson Tyrosine Kinase. *Science* 289: 1938, 2000.

68.   Jacquel A, Herrant M, Legros L et al. Imatinib Induces Mitohondria-dependent Apoptosis of the Bcr-Abl-positive K562 Cell Line and its Differentiation toward the Erythroid Lineage. *FASEB Journal* 17: 2160, 2003.

69.   Druker B. Inhibition of the Bcr-Abl Tyrosine Kinase as a Therapeutic Strategy for CML. *Oncogene* 21: 8541, 2002.

70. Fang G, Kim C, Perkins C et al. CGP57148B (STI571) Induces Differentiation and Apoptosis and Sensitizes Bcr-Abl-positive Human Leukemia Cells to Apoptosis due to Antileukemic Drugs. *Blood* 96 (6): 2246, 2000.

71. Waxman D, Schwartz P. Harnessing Apoptosis for Improved Anticancer Gene Therapy. Cancer Research 63: 8563, 2003.

72. Benito A, Silva M, Grillot D et al. Apoptosis Induced by Erythroid Differentiation of Human Leukemia Cell Lines is Inhibited by Bcl-X_L. *Blood* 87 (9): 3837, 1996.

73. Nimmanapalli R, O'Bryan E, Huang M et al. Molecular Characterization and Sensitivity of STI-571 (Imatinib Mesylate, Gleevec)-resistant, Bcr-Abl-positive, Human Acute Leukemia Cells to SRC Kinase Inhibitor PD180970 and 17-Allylamino-17-demethoxygeldanamycin. *Cancer Research* 62: 5761, 2002.

74. Kreuzer K, le Coutre P, Landt O et al. Preexistence and Evolution of Imatinib Mesylate-resistant Clones in Chronic Myelogenous Leukemia Detected by a PNA-based PCR Clamping Technique. *Ann Hematol* 82: 284, 2003.

75. O'Dwyer M, Mauro M, Kurilik G et al. The Impact of Clonal Evolution on Response to Imatinib Mesylate (STI571) in Accelerated Phase CML. *Blood* 100 (5): 1628, 2002.

76. Rosee P, Corbin A, Stoffgren E et al. Activity of the Bcr-Abl Kinase Inhibitor PD180970 against Clinically Relevant Bcr-Abl Isoforms That

Cause Resistance to Imatinib Mesylate (Gleevec, STI571). *Cancer Research* 62: 7149, 2002.

77.   Gorre M, Mohammed M, Ellwood K et al. Clinical Resistance to STI-571 Cancer Therapy Caused by BCR-ABL Gene Mutation or Amplification. *Science 293: 876, 2001.*

78.   Barthe C, Cony-Makhoul P, Melo J et al. Roots of Clinical Resistance to STI-571 Cancer Therapy. *Science* 293: 2163a, 2001.

79.   Weisenberg E, Griffin J. Mechanism of Resistance to the ABL Tyrosine Kinase Inhibitor STI571 in BCR/ABL-transformed Hematopoietic Cell Lines. *Blood* 95 (11): 3498, 2000.

80.   Ricci C, Scappini B, Divovsky V et al. Mutation in the ATP-binding Pocket of the ABL Kinase Domain in an STI571-resistant BCR/ABL-positive Cell Line. *Cancer Research* 62: 5995, 2002.

81.   Dykxhoorn D, Novina C, Sharp P. Killing the Messenger: Short RNAs that Silence Gene Expression. *Nature Reviews: Molecular Cell Biology* 4: 457, 2003.

82.   Poogin M, Dreyfus M, Hohn T. mRNA Enigmas: The Silence of the Genes. *Int Arch Biosci*: 1023, 2001.

83.   Manfredini R, Capobianco M, Trevisan F et al. Antisense Inhibition of Bax mRNA Increases Survival of Terminally Differentiated HL60 Cells. *Antisense & Nucleic Acid Drug Development* 8: 341, 1998.

84.   Kurreck J. Antisense Technologies. *Eur. J Biochem* 270 : 1628, 2003.

85. Xu Y, Zhang H-Y, Thormeyer D et al. Effective Small Interfering RNAs and Phosphorothioate Antisense DNAs have Different Preferences for Target Sites in the Luciferase mRNAs. *Biochemical and Biophysical Research Communications* 306: 712, 2003.

86. Liu Q, Rand T, Kalidas S et al. R2D2, a Bridge Between the Initiation and Effector Steps of the Drosophila RNAi Pathway. *Science* 301: 1921, 2003.

87. Mukai T, Sekiguchi M. Gene Silencing in Phenomena Related to DNA Repair. *Oncogene* 21: 9033, 2002.

88. Stevenson D, Jarvis P. Chromatin Silencing RNA in the Driving Seat. *Current Biology* 13: R13, 2003.

89. Smale S. The Establishment and Maintenance of Lymphocyte Identity Through Gene Silencing. *Nature Immunology*. 4 (7): 607, 2003.

90. Bosher J, Labouesse M. RNA Interference: Genetic Wand and Genetic Watchdog. *Nature Cell Biology* 2: E31, 2000.

91. Bushman F. RNA Interference: Applications in Vertebrates. *Molecular Therapy* 7 (1): 9, 2003.

92. Schwarz D, Hutvagner G, Haley B et al. Evidence that siRNAs Function as Guides, Not Primers, in the Drosophila and Human RNAi Pathways. *Mol. Cell* 10: 537, 2002.

93. Bruening G. Plant Gene Silencing Regularized. *Proc. Natl. Acad. Sci.* 95: 13349, 1998.

94. Bass B. Double-Stranded RNA as a Template for Gene Silencing. *Cell* 101: 235, 2000.

95. Carmell M, Xuan Z, Zhang M et al. The Argonaute Family: Tentacles that Reach into RNAi, Developmental Control, Stem Cell Maitenance, and Tumorigenesis. *Genes and Development* 16: 2733, 2002.

96. Grishok A, Tabara H, Mello C. Genetic Requirements for Inheritance of RNAi in C. elegans. *Science* 287: 2494, 2000.

97. Tuschl T. RNA Interference and Small Interfering RNAs. *Chembiochem* 2: 239, 2001.

98. Pickford AS, Cogoni C. RNA-mediated Gene Silencing. *Cellular and Molecular Life Sciences* 60: 871, 2003.

99. Kim V. RNA Interference in Functional Genomics and Medicine. *J Korean Med Sci* 18: 309, 2003.

100. Sledz C, Holko M, de Veer M et al. Activation of the Interferon System by Short-Interfering RNAs. *Nature Cell Biology* 5 (9): 834, 2003.

101. Jackson A, Bartz S, Schelter J et al. Expression Profiling Reveals Off-Target Gene Regulation by RNAi. *Nature Biotechnology* 21 (6): 635, 2003.

102. Chiu Y-L, Rana T. siRNA Function in RNAi : A Chemical Modification Analysis. *RNA* 9: 1034, 2003.

103. Semizarov D, Frost L, Sarthy A et al. Specificity of Short Interfering RNA Determined Through Gene Expression Signatures. *PNAS* 100 (11): 6347, 2003.

104. Chiu Y-L, Rana T. RNAi in Human Cells : Basic Structural and Functional Features of Small Interfering RNA. *Molecular Cell* 10: 549, 2002.

105. Borkhardt A. Introduction: RNA Interference in Cancer Biology and Treatment. *Seminars in Cancer Biology* 13: 249, 2003.

106. Brummelkamp T, Bernards R. New Tools for Functional Mammalian Cancer Genetics. *Nature Cancer* 3: 781, 2003.

107. Deveraux Q, Aza-Blanc P, Wagner K et al. Exposing Oncogenic Dependencies for Cancer Drug Target Discovery and Validation Using RNAi. *Seminars in Cancer Biology* 13: 293, 2003.

108. Nagy P, Arndt-Jovin D, Jovin T. Small Interfering RNAs Suppress the Expression of Endogenous and GFP-fused Growth Factor Receptor (erB1) and Induce Apoptosis in erB1-overexpressing Cells. *Experimental Cell Research* 285: 39, 2003.

109. Wu H, Hait W, Yang J-M. Small Interfering RNA-induced Suppression of MDR1 (P-Glycoprotein) Restores Sensitivity to Multidrug-resistant Cancer Cells. *Cancer Reasearch* 63: 1515, 2003.

110. Li K, Lin S-Y, Brunicardi C et al. Use of RNA Interference to Target Cyclin E-overexpressing Hepatocellular Carcinoma. *Cancer Research* 63: 3593, 2003.

111. Scherr M, Eder M. RNA Interference (RNAi) in Hematology. *Ann Hematol* 83: 1, 2004.

112. Scherr M, Morgan M, Eder M. Gene Silencing Mediated by Small Interfering RNAs in Mammalian Cells. *Current Medicinal Chemistry* 10: 245, 2003.

113. Li M-J, McMahon R, Snyder D et al. Specific Killing of Ph+ Chronic Myeloid Leukemia Cells by a Lentiviral Vector-Delivered Anti-bcr/abl Small Hairpin RNA. *Oligonucleotides* 13: 401, 2003.

114. Daheron L, Salmeron S, Patri S et al. Identification of Several Genes Differentially Expressed During Progression of Chronic Myelogenous Leukemia. Leukemia 12: 326, 1998.

115. Merx K, Muller MC, Kreil S et al. Early Reduction of Bcr-Abl mRNA Transcript Levels Predicts Cytogenetic Response in Chronic Phase CML Patients Treated with Imatinib after Failure of Interferon – α. *Leukemia* 16: 1579, 2002.

116. Tuschl T, Borkhardt A. Small Interfering RNAs : A Revolutionary Tool for the Analysis of Gene Function and Gene Therapy. *Molecular Interventions* 2 (3): 158, 2002.

117. Barnes D, Melo J. Management of Chronic Myelogenous Leukemia: Targets for Molecular Therapy. *Sem. Hematol.* 40 (1): 34, 2003.

118. Martiat P, Lewalle P, Taj A et al. Retrovirally Transduced Antisense Sequences Stably Suppress P210[BCR-ABL] Expression and Inhibit the Proliferation of Bcr/Abl-Containing Cell Lines. *Blood* 81 (2): 502, 1993.

119. Kerr JF, Wyllie AH, Currie AR. Apoptosis: a Basic Biological Phenomenon with Wide-ranging Implications in Tissue Kinetics. *Br. J. Cancer.* 26 (4): 239, 1972.

120. Cohen G. Caspases: The Executioners of Apoptosis. *Biochemie J.* 326: 1, 1997.

121. Carmody RJ, Cotter TG. Signalling Apoptosis: A Radical Approach. *Redox Rep.* 6 (2): 77, 2001.

122. Fridman JS, Lowe SW. Control of Apoptosis by p53. *Oncogene* 22 (56): 9030, 2003.

123. Chao D, Korsmeyer S. Bcl-2 Family : Regulators of Cell Death. *Annu. Rev. Immunol.* 16 : 395, 1998.

124. Cory S, Huang D, Adams J. The Bcl-2 Family: Roles in Cell Survival and Oncogenesis. *Oncogene* 22: 8590, 2003.

125. McGahon A, Bissonette R, Schmitt M et al. Bcr-Abl Maintains Resistance of Chronic Myelogenous Leukemia Cells to Apoptotic Cell Death. *Blood* 83 (5): 1179, 1994.

126. Amarante-Mendes G, Kim C, Liu L et al. Bcr-Abl Exerts its Antiapoptotic Effect Against Diverse Apoptotic Stimuli through Blockage of Mitochondrial Release of Cytochrome C and Activation of Caspase-3. *Blood* 91 (5): 1700, 1998.

127. Hsu Y, Wolter K, Youle R. Cytosol-to-membrane Redistribution of Bax and Bcl-X_L During Apoptosis. *Proc. Natl. Acad. Sci.* USA 94: 3668, 1997.

128. Benekli M, Baer M, Baumann H et al. Signal Transducer and Activator of Transcription Proteins in Leukemias. *Blood* 101 (8): 2940, 2003.

129. Horita M, Andreu E, Benito A et al. Blockade of the Bcr-Abl Kinase Activity Induces Apoptosis of Chronic Myelogenous Leukemia Cells by Suppressing Signal Transducer and Activator of Transcription 5-dependent Expression of Bcl-$_{XL}$. *J. Exp. Med.* 191 (6): 977, 2000.

130. Deora A, Miranda M, Rao A. Down-modulation of P210$^{Bcr-Abl}$ Induces Apoptosis/Differentiation in K-562 Leukemic Blast Cells. *Tumori* 83: 756, 1997.

131. Vigneri P, Wang J. Induction of Apoptosis in Chronic Myelogenous Leukemia Cells through Nuclear Entrapment of Bcr-Abl Tyrosine Kinase. *Nature: Medicine* 7 (2): 228, 2001.

132. Jonuleit T, van der Kuip H, Miething C et al. Bcr-Abl Kinase Down-regulates Cyclin-Dependent Kinase Inhibitor p27 in Human and Murine Cell Lines. *Blood* 96 (6): 1933, 2000.

133. Ravandi F, Kantarjian H, Talpaz M et al. Expression of Apoptosis Proteins in Chronic Myelogenous Leukemia. *Cancer* 91 (11): 1964, 2001.

134. Baker EJ, Ichiki AT, Hodge JW et al. PMA-treated K-562 Leukemia Cells Mediate a TH2-specific expansion of CD4+ T Cells In Vitro. *Leuk Res.* 24 (12): 1049, 2000.

135. Kano Y, Akutsu M, Tsunoda S *et al.* In Vitro Cytotoxic Effects of a Tyrosine Kinase Inhibitor STI571 in Combination with Commonly used Antileukemic Drugs. *Blood* 97 (7): 1999, 2001.

136. Hodge JW, Wust CJ, Ichiki AT et al. Antibodies to Specific Cell Surface Antigens of a Human Leukemia Cell Line, K-562, Transduce Negative Growth Signals. *Ann N Y Acad Sci.* 628: 165, 1991.

137. Buss J, Neuzil J, Gellert N et al. Pyridoxal Isonicotinoyl Hydrazone Analogs Induce Apoptosis in Hematopoietic Cells Due to Their Iron-Chelating Properties. *Biochem. Pharmacol.* 65: 161, 2003.

138. Kobayashi T, Sawa H, Morikawa J et al. Bax-Induction Alone is Sufficient to Activate Apoptosis Cascade in Wild-Type Bax-Bearing K562 Cells, and the Initiation of Apoptosis Requires Simultaneous Caspase Activation. *Int. J. Oncol.* 20: 723, 2002.

139. Chomczynski P, Sacchi N. Single-step Method of RNA Isolation by Acid Guanidinium Thiocyanate-phenol-chloroform Extraction. *Anal Biochem.* 162 (1): 156, 1987.

140. Yang D, Buchholz F, Huang Z et al. Short RNA Duplexes Produced by Hydrolysis with Escherichia coli Rnase III Mediate Effective RNA Interference in Mammalian Cells. *PNAS* 99 (15): 9942, 2002.

141. Fernandes RS, Gorman AM, McGahon A *et al.* The Repression of Apoptosis by Activated Abl Oncogenes in Chronic Myelogenous Leukemia. *Leukemia* 10 (Suppl 2): s17, 1996.

142. Wang H, Prasad G, Buolamwini JK et al. Antisense Anticancer Oligonucleotide Therapeutics. *Curr Cancer Drug Targets* 1 (3): 177, 2001.

143. Zhang Y, Boado RJ, Pardridge WM. In Vivo Knockdown of Gene Expression in Brain Cancer with Intravenous RNAi in Adult Rats. *J Gene Med.* 5 (12): 1039, 2003.

144. Lugo T, Pendergast A, Muller A et al. Tyrosine Kinase Activity and Transformation Potency of *Bcr-Abl* Oncogene Products. *Science* 247: 1079, 1990.

Vitae

Benjamin Eugene Baker was born in Chattanooga, TN, on July 18, 1978. He attended the Senter School in Chattanooga, TN. He completed his secondary education at Notre Dame High School, Chattanooga, TN in May 1996. Mr. Baker continued his education at the University of Tennessee at Knoxville, where he received a Bachelor of Science degree in Ecology and Evolutionary Biology with a minor in English Literature in August 2000. Ben worked as a mathematics teacher at Notre Dame High School in Chattanooga, TN and then as a fieldwork archaeologist for Alexander Archaeological Consultants in Wildwood, GA before resuming his education at the University of Tennessee at Knoxville in the summer of 2001. Mr. Baker accepted a graduate research assistantship in January 2003 at the University of Tennessee Graduate School of Medicine under the tutelage of Dr. Albert T. Ichiki, where he completed a Master of Science degree in May 2004.